Volume n° 4 - from P14 to P36

ITALIA 2004

Field Trip Guide Book - P36

32nd INTERNATIONAL GEOLOGICAL CONGRESS

PALEOGENE AND RECENT VOLCANISM IN THE EASTERN RHODOPES (BULGARIA), AND ON MILOS ISLAND (GREECE), AND RELATED INDUSTRIAL MINERALS

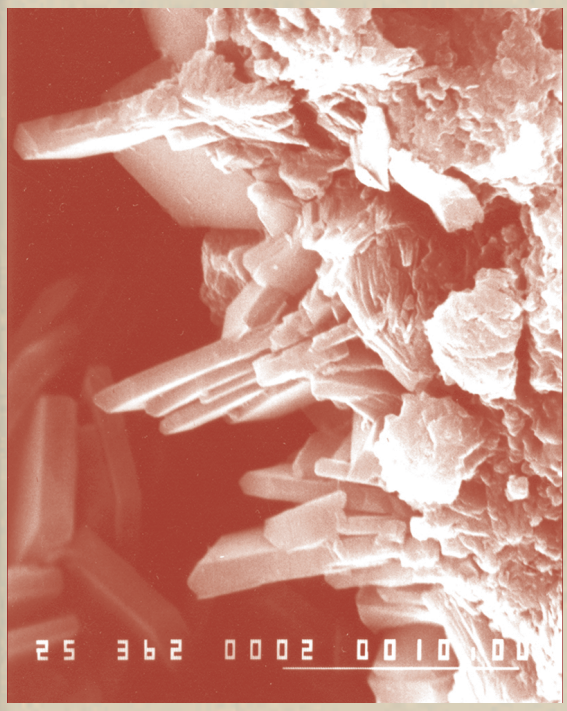

Leader: M. Fytikas

Associate Leader: Y. Yanev

Florence - Italy
August 20-28, 2004

Post-Congress

P36

The scientific content of this guide is under the total responsibility of the Authors

Published by:
APAT – Italian Agency for the Environmental Protection and Technical Services - Via Vitaliano Brancati, 48 - 00144 Roma - Italy

Series Editors:
Luca Guerrieri, Irene Rischia and Leonello Serva (APAT, Roma)

English Desk-copy Editors:
Paul Mazza (Università di Firenze), Jessica Ann Thonn (Università di Firenze), Nathalie Marléne Adams (Università di Firenze), Miriam Friedman (Università di Firenze), Kate Eadie (Freelance indipendent professional)

Field Trip Committee:
Leonello Serva (APAT, Roma), Alessandro Michetti (Università dell'Insubria, Como), Giulio Pavia (Università di Torino), Raffaele Pignone (Servizio Geologico Regione Emilia-Romagna, Bologna) and Riccardo Polino (CNR, Torino)

Acknowledgments:
The 32nd IGC Organizing Committee is grateful to Roberto Pompili and Elisa Brustia (APAT, Roma) for their collaboration in editing.

Graphic project:
Full snc - Firenze

Layout and press:
Lito Terrazzi srl - Firenze

Volume n° 4 - from P14 to P36

32nd INTERNATIONAL GEOLOGICAL CONGRESS

PALEOGENE AND RECENT VOLCANISM IN THE EASTERN RHODOPES (BULGARIA), AND ON MILOS ISLAND (GREECE), AND RELATED INDUSTRIAL MINERALS

AUTHORS:

Y. Yanev *(Bulgarian Academy of Sciences, Sofia - Bulgaria),*
M. Fytikas *(Aristotle University of Thessaloniki, School of Geology)*

WITH PARTICIPATION OF:

R. Ivanova *(Bulgarian Academy of Sciences, Sofia - Bulgaria)*
T. Iliev *(Bulgarian Academy of Sciences, Sofia - Bulgaria)*
S. Gier *(Vienna University - Austria)*

Florence - Italy
August 20-28, 2004

Post-Congress

P36

Front Cover:
Platy Ca-clinoptilolite grown on fine K-clinoptilolite crystals on the wall of the pumice bubble (the black bar is 10μm); Jelezni-Vrata zeolitized tuffs deposit, Eastern Rhodopes. JEOL superprobe 735.

Leader: M. Fytikas
Associate Leader: Y. Yanev

In the Eastern Rhodope mountains, a huge and extended volcanism developed during the Paleogene. In Bulgarian territory, this field trip will focus on two points: a) different types of volcano-clastic products (ignimbrites, fall-out tuffs), and various volcanic massifs (domes, lava flows etc), b) the transformation of these products, by hydrothermal activity or by a quick cooling of the "border" lavas of the volcanic structures and products, into industrial minerals (zeolites or bentonites), or by a quick cooling of the "border" lavas of the volcanic structures and products, we will visit a rhyolitic tuff ring with a diameter of 1,700 m, a gigantic pumice deposit, some great phreato-magmatic craters, spectacular lava –domes and flows, gigantic columnar dikes, and numerous hydrothermal craters. A great variety of hydrothermal and industrial minerals were formed: bentonite, kaolin, barite, silica, alunite, sulpure, manganese, epithermal gold etc., together with an impressive geothermal field. A huge industrial production activity exists, producing more than 1 million tonnes of bentonite and 500,000 tonnes of perlite yearly. We will visit some of the most important and interesting quarries.

The duration of the field trip will be 5 days; the departure point is Sofia (Bulgaria), the arrival point Athens (Greece). Travel will be by airplane and bus. The degree of physical effort is low. Temperatures: 22-30°C.

FIRST PART: Eastern Rhodopes

Regional geological setting

Author: Y. Yanev (Geological Institute, Bulgarian Academy of Sciences)

Introduction

Paleogene volcanic activity in the Eastern Rhodopes (Harkovska et al., 1989; Dabovski et al., 1991; Yanev et al., 1998a) took place at the end of the Paleogene collision between Eurasian (represented here by the Rhodopes terrain) and Apulian plates during the final closure of the Thetys Ocean in the area. The blocking of the subduction during the continental collision, and the following crustal thickening, led to orogenic uplifting, exhumation of metamorphic cores and the formation of graben basins along their peripheries. Sedimentation, firstly continental, more recently marine, began in the Middle (?)–Late Eocene. The volcanic activity started after the beginning of the sedimentation, lasting to differing extents in the different parts of the basin, and continued until the

Figure A - Itinerary of the 1st day (dotted) of the P-36 excursion (for the 2nd day see Fig. B).

Volume n° 4 - from P14 to P36

Volume n° 4 - from P14 to P36

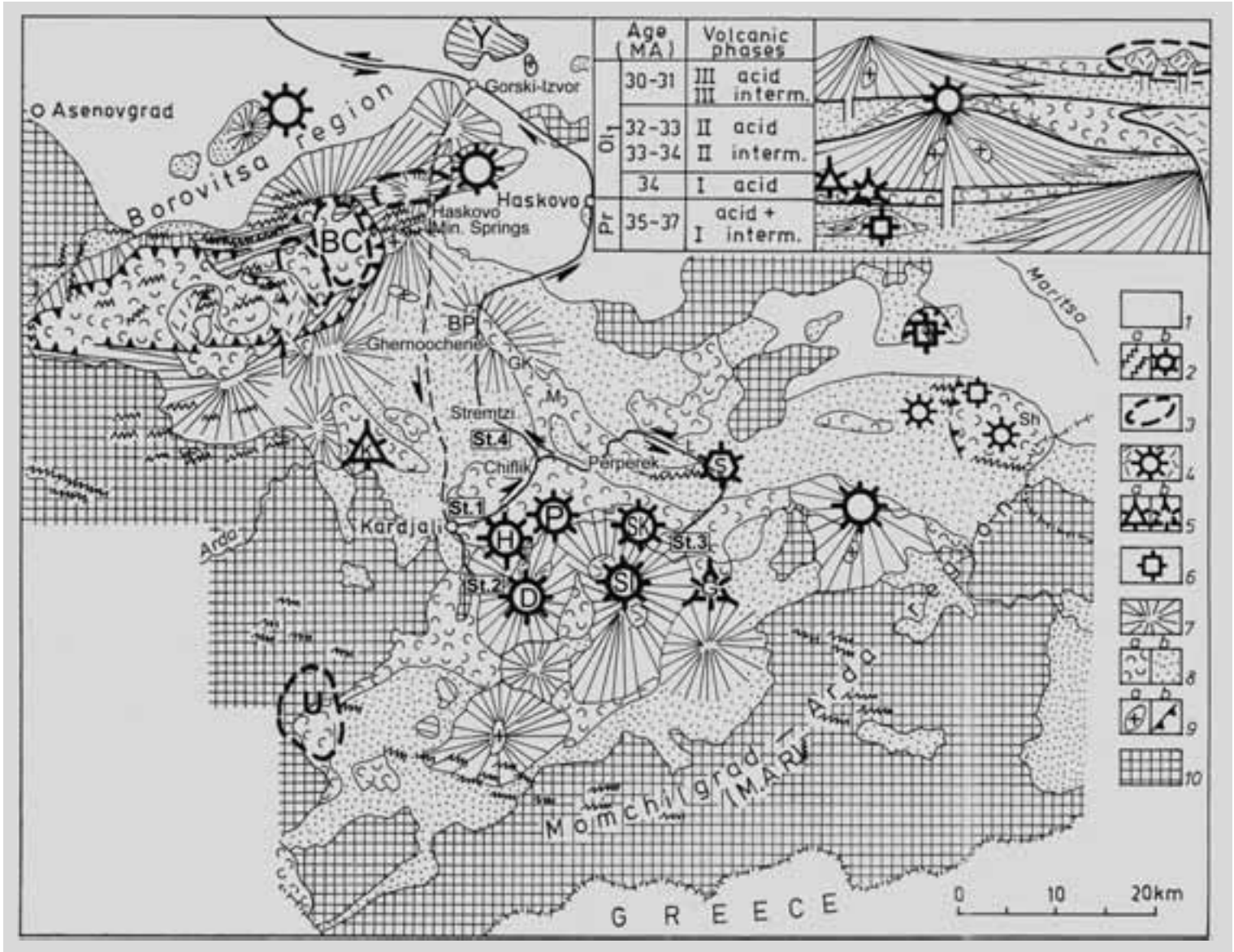

Figure B - Simplified map of the Eastern Rhodopes volcanic area (Yanev, 1998) with the itinerary of the 1st (dashed line) and 2nd day (solid line); the stops (from St.1 to St.4) are also shown. In the corner: schematic stratigraphic column of the Priabonian (Pr) and Early Oligocene (Ol_1) phases. Key: (1) Neogene-Quaternary cover; Upper Oligocene: (2a) dykes (29-25.5 Ma) and (2b) volcano; Lower Oligocene: (3) acid dome-clusters of 3rd phase, (4) acid volcanoes of 2nd phase, (5a) acid explosive volcano and (5b) domes of the 1st phase; (6) Priabonian acid volcano; (7) intermediate volcanoes of different phases; (8a) acid tuffs and ignimbrites of different phases, (8b) Priabonian-Oligocene sediments; (9a) plutons and (9b) caldera faults; (10) crystalline basement. Volcanoes: (D) Dambalak, (H) Hisar, (K) Kostino (inferred), (P) Perperek, (S) Silen, (SL) St Ilia, (SK) Studen-Kladenetz, (Y) Yabalkovo; (U) Ustra dome-cluster; (BC) Borovitza caldera. Zeolitized tuffs deposits: BP, G, GK, L, M, Sh (see Fig. C).

end of the Early Oligocene.

The volcanic activity was of a cyclical character, that is, as 4 intermediate phases which alternated with 5 acid phases (the 1st of which is Priabonian, and all the rest are Early Oligocene), which are traditionally labeled as the 1st intermediate phase, 1st acid phase, etc. (Ivanov, 1960), and their age (according to Lilov et al., 1987) is indicated in Fig. B. The individual volcanoes are built up of the products of one or (maximum) two phases (intermediate and acid), but the acid pyroclastics are normally distributed over the whole volcanic area and this creates a picture of overall distribution of each phase. The Eastern Rhodopes volcanic area has been divided into two regions: northern, Borovitza, and southern – Momchilgrad-Arda (Fig. B).

Deposits of perlite (Goranov et al., 1960; Yanev, 1987), both of zeolitized (Alexiev et al., 1997; Raynov et al., 1997) and adularized pyroclastics, and some bentonite deposits are related to the acid volcanism (Fig. C). The zeolite deposits are mainly clinoptilolite, and just two are mordenite. The alunite and the most important bentonitized tuff deposits, as well as some agate occurrences, associate with the intermediate volcanism. Only perlites, zeolitized and bentonitized pyroclastics are currently exploited, and they are the objects of the present field trip.

The intermediate volcanoes are shield-like or stratovolcanoes, with diameters of up to 25-30 km, and current elevation of up to 700-800 m. They are built up of basaltic andesites and andesites, or by shoshonites, latites, and ultrapotassic latites. Single flows of basalts or trachybasalts are rarely present. Some of the volcanoes are intruded by monzonitoid plutons. The volcanic rocks contain phenocrysts (in quantities of up to 20-30%) of andesine-bytownite, enstatite, augite, biotite, Ti-magnetite, sometimes – amphibole, and in more basic varieties – olivine. The texture of the matrix is pilotaxitic, hyalopilitic, shoshonitic or trachytic. The lava and agglomerate flows are interbeded by pumice to ash pyroclastics and epiclastics in proximal areas. The pyroclastics are bentonitized and are the object of the present field trip (Stop 2). Only epiclastic and sedimentary deposits (mudstones, sandstones, and limestones) are observed in the distal areas. The volcanoes developed during the 1st intermediate phase are located mainly in the northern volcanic region, these of the 2nd phase – mainly in the southern region where the most important bentonite deposits are situated. The 3rd and 4th phases are represented by one volcano each, as both are located in the southern region.

Acid volcanoes are of several types (Yanev, 1998): tuff rings, that produced only pyroclastic flows; dome volcanoes, built by intergrown domes with pyroclastics in between and sometimes with short and thick flows; dome clusters, often situated within calderas, that do not form central volcanoes, but each dome is a monogenic volcano. A transitional type between dome volcanoes and dome clusters has also been identified (Studen-Kladenetz volcano, Stop 3). The acid volcanics are mainly rhyolites, trachyrhyolites to trachydacites, rarely – dacites. Normally they contain phenocrysts up to 10% but there are also domes very rich in phenocrysts (over 50%). The phenocrysts are of quartz (in more alkaline rocks quartz appears at SiO_2>73%wt), oligoclase-andesine (rarely more basic), sanidine, biotite and very rare – anortoclase. Amphibole (edenite or Mg-hornblende) is present in some volcanics, whereas diopside has been found in others (crystallization temperatures for the first are <710-720°C depending on SiO_2 rock content, for the second – they are higher than 710-720°C; Yanev, 1998). The ground mass is granoblastic (in subvolcanic bodies), spherolitic, or felsitic, consisting of feldspar and quartz, or tridimite (Dimitrov et al., 1984). Microlithes of feldspars and biotite are also present. Water-containing (2-6%) volcanic glasses (perlites), that are object of the present field trip (Stop 3), formed in the periphery of the lava bodies due to supercooling (Yanev, 1987). Some hundred bodies of perlites are known in the Eastern Rhodopes, and none of them consists of low-water glass (obsidian). This is one of the reasons for considering perlites as directly resulted from the

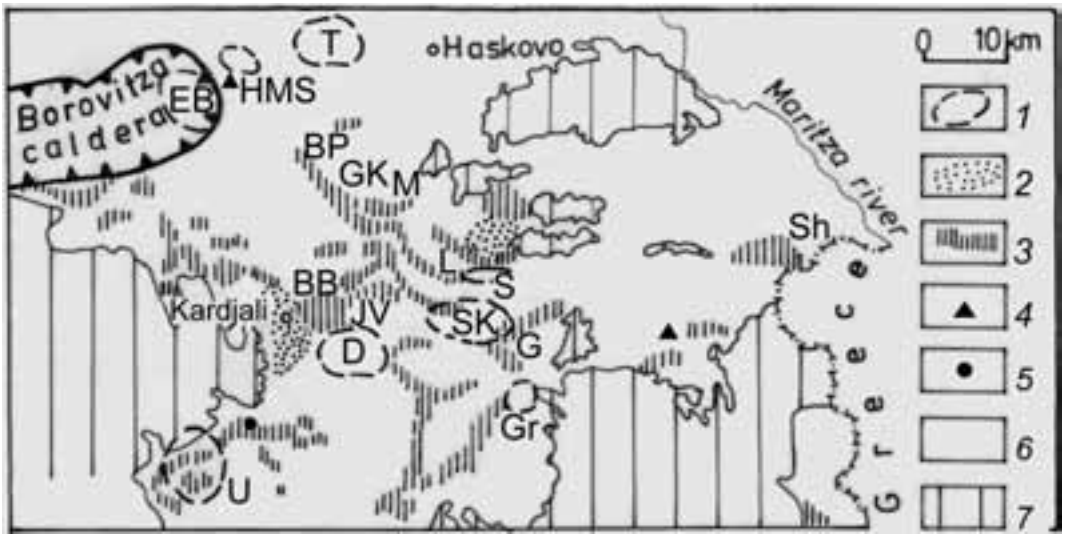

Figure C - Distribution of the principal industrial minerals in the Eastern Rhodopes Paleogene volcanic area. Key: (1) area of the perlite deposits (D, Dambalak, Hisar, Perperek and St. Ilia volcanoes; EB, Eastern Bororvitza; Gr, Geren; HMS, Haskovo Mineral Springs; S, Silen volcano; SK, Studen-Kladenetz volcano; T, Tatarevo; U, Ustra), (2) bentonitized tuffs, (3) zeolitized tuffs deposits (BB, Belia-Bair, BP, Beli-Plast, G, Golobradovo, GK, Gorna-Krepost, JV, Jelezni-Vrata and M, Most -clinoptilolite; L, Liaskovetz and Sh, Sheinovetz-mordenite), (4) alunite deposits, (5) adularized tuffs, (6) Paleogene volcanics and sediments, (7) crystalline basement.

cooling of water-containing lava, not from additional obsidian hydration. The lava bodies were emplaced either at shallow depth in water-containing sediments, or were erupted on the sea bottom, which prevented lava from intensive bubble growth and pumice formation. The pumiceous parts of the lava bodies formed in the case of subaereal eruption probably have been eroded.

A progressive decreasing in the volcanic explosivity is typical of the acid volcanic activity. *The 1st acid Early Oligocene phase* was mainly explosive, and the inferred volcanic center was Kostino, from which only pyroclastic flows erupted (Yanev and Bardintzeff, 1997): one ash flow in the base was followed by two pumice flows which deposited low- to moderately-welded ignimbrites. They extended only to the north of the Arda River. Coastal reefs prevented them from farther southward transportation, and to the south of the reefs, only fall-out tuffs (presently bentonitized), alternating with limestones, are to be found. Nord of the reefs, the limestones are absent, and only fall-out tuffs are deposited (now zeolitized - Stop 4). *The 2nd acid Early Oligocene phase* is paroxysmal of the Eastern Rhodopes volcanism. In the northern volcanic region, the violent explosions resulted in generation of numerous pyroclastic flows, which spread even into some parts of the southern region. They are accompanied by thick fall-out tuffs, produced by the same eruptions that led to the nested Borovitza caldera subsidence (30 x 15 km). The pyroclastic flow deposits within the caldera are high-grade ignimbrites, and outside the caldera – low-grade to non-welded ignimbrites (presently zeolitized - Stop 1). The explosive products are spread far away from the Eastern Rhodopes (in Thrace, to the south of the Balkan Mountains, and probably as far as in the Carpathians and Ukraine). Numerous high-Si rhyolite domes with perlite peripheries were emplaced after the caldera collapse. In the southern region, this phase is represented by some trachyrhyolite to trachydacite lava dome volcanoes, which top the large latite volcanoes along the Arda River valley that had developed during the former 2nd intermediate phase (e.g. Dambalak volcano, Stop 2). Some small volcanoes (Hisar near the town of Kardjali – Stop 1, Perperek, and Studen-Kladenetz volcanoes – Stop 3), are located in their northern foot. Many acid domes and flows have perlite peripheries.

The 3rd acid Early Oligocene phase is of restricted volume, and is represented mostly by lava varieties. Part of the acid volcanoes crowning the intermediate ones, also belongs to this phase, as well as the Ustra dome cluster (high-Si rhyolites), to which the largest perlite deposit, Schupenata-Planina (Broken Hill),

is connected. Acid epiclastics and limestones were deposited during this phase in the distal area.
In the southern region, the products of the above mentioned phases are covered by alluvial deposits in an E-W trending valley more than 70 km long (called Paleo-Arda). These are rhyolite conglomerates at the base, cross-bedded sandstones and mudstones covered by the products of the Silen rhyolite volcano, which was formed during *the 4th acid phase*. This volcano is composed of E-W aligned domes with perlite peripheries. Probably during this phase, and also during the Late Oligocene, the metamorphic basement and the overlaying volcanic products were intruded by subvolcanic rhyolite bodies and 130°-trending dyke swarms.
The proposed genetic model for the Eastern Rhodopes volcanism is discussed in Yanev et al. (1998a) and Yanev (2003).

Field itinerary

DAY 1

Beginning from Sofia (Fig. A), the field trip route crosses the Pliocene Sofia depression (filled with lake deposits, and rich in thermal mineral springs), and the Ihtiman crystalline terrain, with numerous Upper Cretaceous granites belonging to the Srednogorie volcanic island arc system (Dabovski et al., 1991). Epithermal porphyry-cupper deposits, associated with the Cretaceous magmatism, can be seen on the left. About 80 km from Sofia, the road enters the Upper Thracian depression, filled with Paleogene marine and Neogene lake deposits laying over volcanic arc products. The road goes to the north of Plovdiv, emplaced on hills built up by Upper Cretaceous monzonites. At the village of Gorski-Izvor (215 km from Sofia), we enter the Eastern Rhodopes volcanic area (Fig. B): the northernmost and the oldest (Bartonian) latites of Yabalkovo volcano (Yanev et al., 1998b) can be seen on the left, and Priabonian latites (1st intermediate phase) are exposed to the south of Gorski-Izvor village.
Rhyolite domes (age 29.5-30.4 Ma; SiO_2=70.34-75.90, Na_2O=2.43-3.80, K_2O=4.78-5.04%wt - Yanev and Pecskay, 1997), with perlite periphery (the first perlites were described in Bulgaria by Bontscheff, 1897), are crossed near the village of Haskovo Mineral Springs. They are located in the eastern periphery of the Borovitza region. The mountains visible into the distance on the right are built of Priabonian latites and Lower Oligocene ultrapotassic latites (32-33.32 Ma; SiO_2=57.14-59.34, Na_2O=2.01-2.67, K_2O=5.20-6.20%wt), from the periphery of the Borovitza caldera. The Priabonian latites (hydrothermally altered in many places) are also exposed along the road to the town of Kardjali. They host the large Spahievo Pb-Zn-Au ore district (including some deposits of alunites, turquoise, etc.). Flysch deposits from the deepest parts of the Priabonian basin, with submarine slides and intralayer deformations, are exposed between the village of Chernoochene and the town of Kardjali. They are covered by limestones, also Priabonian in age (in the distance on the left), or by the pyroclastic flow deposits of the 1st Early Oligocene acid phase (seen on the right).

DAY 2

The bentonitized tuffs of the Dobrovoletz deposit are exposed to the east of Kardjali, eastwards of the road (in front of the Pb-Zn metallurgic factory), at the beginning of the trip. They are covered by pyroclastic flow deposits (three flow units), and fall-out tuffs of the 2nd acid phase described in Stop 1. The lowest flow deposit is NW-dipping and laminated, probably as a result of passing over a barrier (here – coral reefs), similarly to the pyroclastic flow deposit in VTTS (Alaska), as described by Fierstein and Hildreth (1992). Then our route crosses the area of the Jelezni-Vrata zeolite deposit.

Stop 1:

Zeolite deposit "Jelezni-Vrata" ("iron door")
Authors: ***Y. Yanev, R. Ivanova. and Tz. Iliev (Geological Institute, Bulgarian Academy of Sciences).***

The deposit is located 4 km to the east of Kardjali (Fig. 1-1) on the Arda River bank, and occupies an area of about 16 km^2, close to the trahcydacite volcano Hisar, which is capped by a dome flow (SiO_2= 66.54-68.57, Na_2O=3.7-4.31, and K_2O=5.64-6.42). The complex latite-trachydacite volcano Dambalak (trachybasalts to latites with SiO_2 = 50.85 - 62.26, Na_2O = 1.86 - 4.50, and K_2O = 2.0 - 4.02 %wt; trachydacites having SiO_2 = 70.65 - 71.85, Na_2O = 3.64 - 4.11, and K_2O = 5.26 - 5.79%wt) are located on the opposite bank of the Arda River (Fig. B). The deposit includes the zeolitized (clinoptilolitized) explosive products (non-welded to low-grade ignimbrites and fall-out tuffs), of the 2nd acid phase. The deposit has been

Volume n° 4 - from P14 to P36

exploited over the last 50 years, as the mined raw material is used in the cement industry – as a clinker addition for lightening and improving the cement-binding properties. As a zeolite raw material the deposit has been found by Prof. B. Alexiev (Alexiev, 1968; Djourova and Aleksiev, 1990), and as such can be used as a sorbent (inclusive of radionuclides), for oxygen enrichment in metallurgy, as a dietary supplement in animal husbandry, as a mineral soil, a deodorant, etc. (Raynov et al., 1997).

Geological background

The zeolitized pyroclastics are underlayed by the products of the 2nd intermediate phase erupted by the Dambalak volcano, represented here by (from the bottom to the top): (1) yellow bentonitized latite ash to lapilli-sized pumice tuffs (the same as at Stop 2), consisting mainly of altered pumice fragments. Plagioclase, rarely K-feldspar, dense lava fragments (probably of latite), and adularized perlite clasts are also present. The pumice is replaced by clay mineral, zeolites (clinoptilolite and less mordenite), calcite and adularia (Fig. 1-2). The <2μ fraction consists of mixed-layered illite/smectite. The quantity of illite in the mixed layers is estimated on the basis of the difference between positions of the smectite reflection at 5 and 8.5° 2θ ,and near 16 to 17° 2θ, and after solution with ethylene glycol (according to the Table 8.3, Moore and Reynolds, 1997), is about 15%. The structural formula of I/S, based on a formula unit of 11 oxygens (as H_2O is not considered), is: $(Ca_{0.092}Na_{0.025}K_{0.123})$ $(Al_{1.241}Mg_{0.368}Fe^{3+}_{0.361}Ti_{0.027})$ $(Si_{3.977}Al_{0.023}O_{10})(OH)_2$ (average from 8 microprobe analyses). (2) Bright green latite epiclastics. They contain rounded latite clasts, up to 1 cm in size (single clasts can be up to 5-10 cm), grading upwards into blocks (up to 50 cm), and free crystals of plagioclase, pyroxene, sanidine, and biotite. Single altered pumice fragments are also present. The matrix consists of calcite, smectite, and celadonite, as the celadonite coats the clasts and the walls of the small cavities filled with silica, and replaces biotite phenocrysts

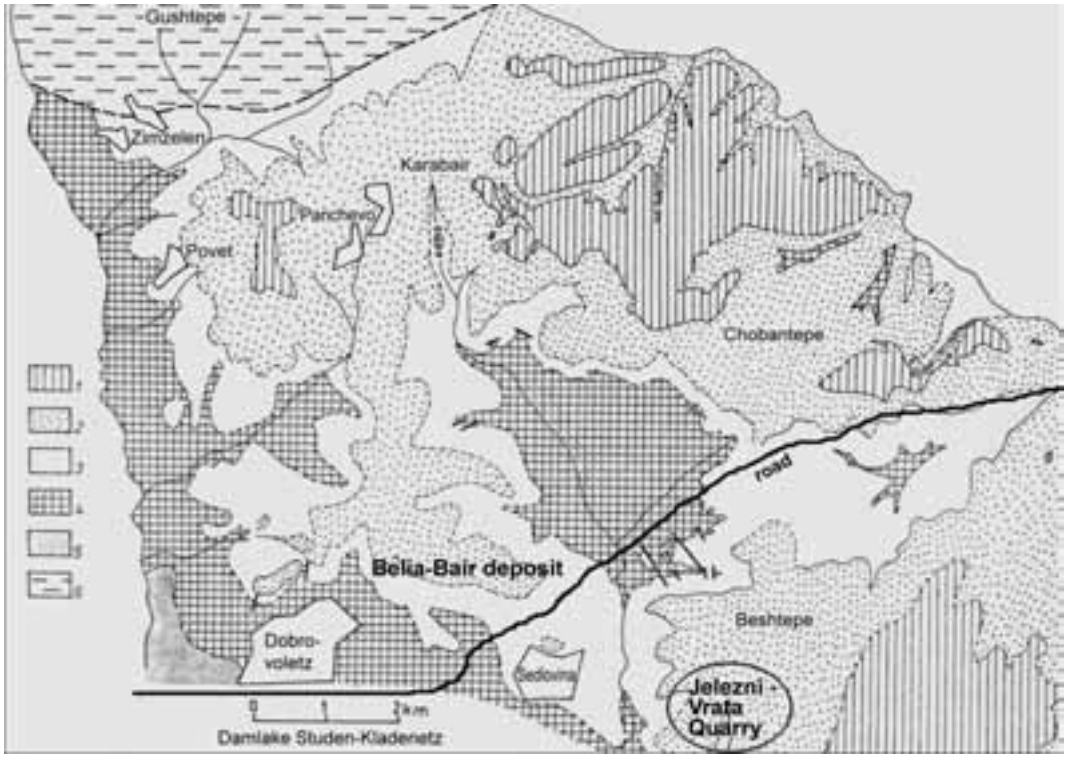

Figure 1.1 - Geological map of Jelezni-Vrata (Stop 1) and Belia-Bair zeolitized tuffs deposits (mapped by Yanev in 1963 on scale 1:10 000). Key: pyroclastic rocks of the 2nd acid phase: (1) the deposits cover (upper pyroclastic flows and epiclastics), (2) fall-out tuffs and 4th pyroclastic flow, (3) lower three pyroclastic flows; (4) epiclastics and bentonitized tuffs of the 2nd intermediate phase; (5) 1st acid phase; (6) Priabonian limestones..

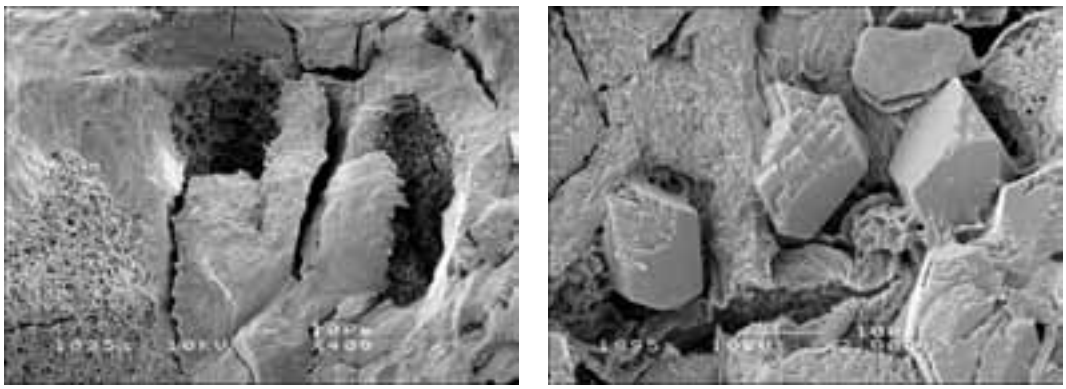

Figure 1.2 - SEM images of bentonitized latite pumice tuff: left, pumice fragment (the tube-like bubbles are still perfectly seen) completely replaced by smectite; right, clinoptilolite and rhomb-like adularia enclosed by smectite.

in the lava fragments. Clinoptilolite and adularia have also been detected. Coral reefs (with horizontal dimensions from several to 100 m), can be seen within the epiclastics, as one large reef is located in the southern part of the quarry (on the dam bank).

The cross-section of the products of the 2nd acid volcanic phase, starting from the bottom, is the following:

1. A bed (up to 1 m thick) of layered pale green fall-out tuffs, composed by fine-lapilli clasts. In many places, it is cut and deformed by the overriding pyroclastic flow (layer 2a). It consists of crystalloclasts (quartz, feldspars, biotite, and amphibole) 0.2-1.2 mm in size, little lithoclasts (spherolitic rhyolites and perlites), and pumices (0.15-0.6 mm) with spherical bubbles. The matrix consists of fine acute glass shards as rarely microfossils can also be seen. All glass shards and pumice clasts are replaced by zeolites, accompanied by clay minerals. Celadonite, giving the greenish color of the rocks, is formed in the central voids of the shards and along the bubble walls in the pumice.

2. Non-welded to low-grade ignimbrites, deposited by three pyroclastic flows (Fig. 1-1), each 7-10 m thick. Individual flow units are separated by either few-centimeter thick layers of fossils containing epiclastics (Djourova and Aleksiev, 1990) or co-ignimbrite ash layers.

2a. a 1-2 m thick layer of basal latite breccia (clast size is 5-10 cm, rarely up to 1 m) lies in the base of the lowest flow deposit. Many clasts of spherolitic rhyolites, perlites, and pumice (0.15-0.6 mm), as well as acute crystalloclasts (0.2-1.2 mm) of quartz, plagioclase, sanidine, and biotite flakes are also presented. All glassy clasts are zeolitized, as in the central voids montmorillonite, carbonate or celadonite is developed. Perlite clasts might have been zeolitized prior to their transportation and deposition as an element of the pyroclastic flows. The matrix is clay-carbonatic, and contains microfossils and zeolitized vitroclasts. Blocks derived from both the underlaying tuffs and coral reefs can often be seen. In the uppermost 0.5 m the breccia fast depletes in large blocks, and grades into the non-welded to low-grade ignimbrites of the 1st flow, which is locally laminated. This basal breccia can be interpreted as either lag-breccia resulted from the collapse of the dense part of the eruptive column (Druitt and Sparks, 1982), and then transported as a pyroclastic flow or lahar (mud flow, composed of clasts derived from the volcano slope, and covered by the following pyroclastic flow). There is no hematization of the underlaying tuffs, which is indicative of "cold" transport and deposition of the described breccia.

2b. the two following flows have hematized basal parts up to 1 m thick (as the hematization also affects the top of the underlaying deposits). By contrast, from the lowermost flow, they show no internal lamination, since they flowed on an already flattened surface.

The three flow deposits are pale pink in color (due to the montmorillonite accompanying zeolites), and are low-grade to non-welded ignimbrites (resulted from their deposition in a shallow marine environment), poorly sorted, and rich in fine-grained pumice (0.47-0.75 mm in size). The main component of their basal part (Fig. 1-3, left) is crystallolithoclastic, including mainly crystalloclasts (0.15-1.5 mm) of quartz (rich in melt inclusions), sanidine, plagioclase, and biotite as well as lithoclasts (up to 0.5 cm in size) - mainly pumice and rhyolite, with less perlite and latite. The

Volume n° 4 - from P14 to P36

matrix is clay-zeolite, in very small quantities. These deposits gradually grade into pumice (up to 1.8 mm in size); ignimbrites (Fig. 1-3, right), containing small amount of crystalloclasts of the above-mentioned types (mainly quartz, sanidine $Or_{66.4\text{-}72.9}Ab_{26.2\text{-}32.6}$, plagioclase $An_{18.8\text{-}39.5}Or_{2.0\text{-}6.5}$, biotite, a little amphibole, magnetite, rarely titanite or zircon); and very small amount of lithoclasts (felsitic and spherolitic rhyolites). The pumice contains both spherical and spindle- to tube-like bubbles. The matrix is in very small quantities and consists of ash-sized glass shards. The lava temperature increases from the 1st to the 3rd flow and is 700, 720 and 740 °C, respectively (according to the two-feldspar geothermometer of Fuhrman and Lindsley, 1988).

3. Thinly-bedded (layers up to 5 cm thick) ash fall-out tuffs, 5-7 m in total thickness, pale pink in color, with ripple-marks of vermicular and other types. They consist of acute glass shards and tiny crystalloclasts (mainly of quartz and feldspars) but rarely pumice (Fig. 1-4). Clay lenses and nodules, concretions 5-6 cm in diameter, and 1-2 cm-sized black nodules of psilomelan with different Mn/Ba ratios (Fig. 1-4), can be seen locally within the tuffs as all they enclose glass shards. The ripple-marks are rich in rose montmorillonite.

4. The ignimbrites (more than 20 m thick) deposited by the 4th flow have uneven, locally hematized bottom. They are also low-grade to non-welded, but compared with the lower flow deposits, are enriched in coarse-grained pumice clasts (1-2 cm in size), often rounded. They are gray to pale green in color, and contain lenses enriched in chloritized biotite.

5. Fall-out tuffs (more than 30-40 m thick) similar to those described in paragraph 3, but grayish white in color and more thickly bedded (the layers are up to 10 cm thick). Small coral reefs appear in the upper parts.

The topmost level of the 2nd, 3rd and 4th flow deposits, as well as the fall-out tuffs located between them (paragraphs 2-4 of the described section) are mined in the quarry. The whole-rock chemistry of these units is presented in Table 1-1.

6. Several meters-thick, not well individualized, pyroclastic flow deposits. The composition of these ignimbrites is identical to these of the underlaying pyroclastic flow deposits, but some of them are enriched in biotite-pyroxene latite clasts. They have uneven boundaries with, or interbed with, the top of the underlaying fall-out tuffs (paragraph 5).

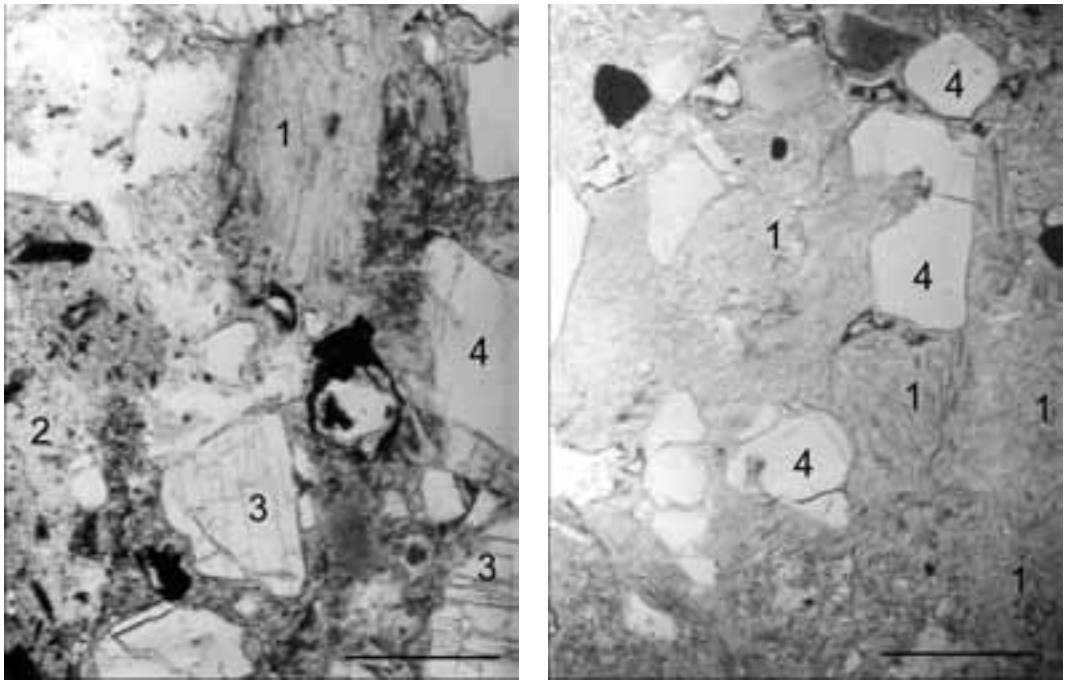

Figure 1.3 - Microphotographies of ignimbrite samples from Jelezni-Vrata zeolite deposit (the samples are artificially colored): left, the basal part and right, the middle part of the pyroclastic flow deposits. Key: (1) zeolitized pumice clast, (2) latitic clast, (3) feldshpars and (4) quartz clasts in the zeolitized matrix. // N. The bar is 0.5cm.

Upwards, with no clear boundary, they grade into latite epiclastics.

7. The latitic epiclastic rocks are poorly-sorted and locally thickly-bedded. They contain varying types of latite clasts (inclusively red in color resurgent ones), up to 5-10 cm in size, great amounts of pumice clasts, and single rhyolite and perlite fragments. The crystalloclasts of feldspars, pyroxene, and biotite are not very abundant. The matrix is almost lacking, but sometimes zeolites have crystallized between the clasts. They also contain lenses (up to 10-15 m long) of bioclastic limestones and coral reefs, very often silificated. Latite epiclastics are more than 100 m thick.

The inferred vent region for these pyroclastic flow deposits is Borovitza caldera (Yanev and Bardintzeff, 1996), located 25 km to the northeast of the deposit. The pyroclastic flows stopped at the northern foot of the Dambalak volcano that had risen during the former 2nd intermediate phase. The lamination of the lowermost flow (to the NW) and deformations in its base are indicative of the flow direction. Moreover, the ignimbrites contain quartz crystalloclasts, while the lavas produced by the closely located acid volcanoes Hisar and Dambalak do not contain quartz phenocrysts (Yanev, 1998). The cone of the trachydacite volcano Hisar, rising just next to the quarry, is built up of coarse block and ash flow deposits wedged into the fine-grained fall-out tuffs. Impact structures of blocks erupted from this volcano are preserved in the tuffs of the zeolite deposit. The latite epiclastics covering the deposit materials have some of the features of the lag-breccia (Druitt and Sparks, 1982), which derived from collapse of the dense part of the eruptive column and was deposited close to the volcano vent (e.g. during the acid activity of the Dambalak volcano). On the other hand, these epiclastics can be deposited from dense mud flows, dragging a mixture of latite fragments (including bombs), and loose acid tephra down from the flanks of the same volcano. The presence of the coral reefs is somehow indicative of the second hypothesis.

Zeolitization

All glassy shards (vitroclasts and pumices), constituting the pyroclastic rocks and the matrix of the epiclastic rocks, are replaced by clinoptilolite, accompanied by opal-crystobalite-trydimite (opal-CT), Ca-montmorillonite, illite (celadonite has been identified only in the lower pyroclastic layer) and probably adularia. Small quantities of lomontite and gmelinite (?) are detected in the lower pyroclastic flow unit, and needles of mordenite – in the 4th flow unit. The quantities of the glass replacing minerals and crystalloclasts are presented in Table 1-2: the highest quantity of the clinoptilolite is registered in the fall-out tuffs, and this of the crystalloclasts – in the 1st flow deposit.

The shape of both vitro- and pumice clasts is fully preserved (Fig. 1-4). Most often they are zonally replaced: a thin montmorillonite or illite film is formed along their outlines, as well as along the bubble walls in the pumice; the periphery of the shards is replaced by tiny clinoptilolite crystals with K as the main exchangeable cation; the inner part of the vitroclasts is replaced by heulandite-type platy crystals (1-2 to 10-12 μm, rarely up to 20 μm in size, photo on the front cover page), with Ca as the most abundant exchangeable cation. The clay minerals form very small drops between the clinoptilolite crystals. These minerals give the characteristic color of the zeolitized tuffs – celadonite gives the grey color of the lower layer, and the Fe-poor montmorillonite provides the pink and white color of the other zeolitized pyroclastic rocks. The opal-CT is hard to recognize, as it forms only globules or irregular grains between the clinoptilolite crystals in the vugs. The ignimbrite matrix is replaced by the cryptocrystalline aggregate of the above mentioned minerals.

Data obtained from the bore-hole exploration of a neighboring area (Belia-Bair deposit), show the following average composition (calculated on the base of 42 samples), from a 90 m thick section: clinoptilolite 52.8%, montmorillonite 7.8%, illite 4%, opal-CT 4.3%, calcite 0.9%, adularia (including sanidine) 17.4%, quartz 4.6%, plagioclase 7.5%; CEC measured in 5 samples varies from 88 to 129 meq/100g (Raynov et al., 1997). The exchangeable cations of the clinoptilolite (Table 1-3) change gradually from the 1st flow unit to the fall-out tuffs: Ca and Na decrease, K increases. The clinoptilolite passes from K-Na type in the 1st flow, to a Na-K one in the fall-out tuffs.

The zeolitization of the volcanic glass from the thick pyroclastic successions, is low-temperature alteration occurring in a slightly alkaline environment of an open hydrological system. However, whether this alteration is a diagenetic process (i.e. <200°C) (Sheppard and Hay, 2001; Utada, 2001), or resulted from the alteration of low-temperature hydrothermal solutions circulated throughout the highly permeable

Volume n° 4 - from P14 to P36

pyroclastic deposits (Gogishvili; 1980; Rainov et al., 1997), is a question still open to debate.

After Stop 1 we will go back to Kardjali, whence our route goes on to Stop 2. Leaving behind the town and crossing the Arda River, the metamorphic basement, covered by Priabonian limestones, is seen in the distance on the right. The Lower Oligocene volcano Dambalak (2nd intermediate phase), crowned by trachydacite lavas (2nd and 3rd acid phases), rises on the left, on the southern bank of the river.

Stop 2:

Bentonite outcrop

Authors: Y. Yanev, R. Ivanova (Geological Institute, Bulgarian Academy of Sciences) and S. Gier (Institute of Petrology, Vienna University).

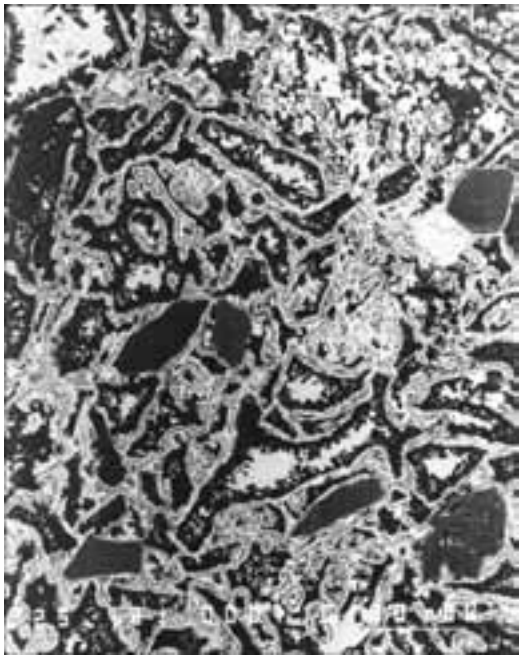

Figure 1.4 - Back scattered electron image of Mn nodule in the zeolitized ash tuff: vitroclasts with central voids replaced by platy K-clinoptilolite crystals (black) and cemented by psilomelan with different Mn/Ba ratio (white, 6 - 6.7; grey, 9 - 13). (1) quartz and sanidine crystalloclasts. The white bar is 100 µm.

This bentonite outcrop is located 4 km to the south of the town of Kardjali (Fig. B), in the western foot of the Lower Oligocene volcano Dambalak. A latite sheet (SiO_2=57.60, Na_2O=3.82, K_2O=3.71%wt), having a finely columnar jointed base, is visible to the north. The latite contains small amount of phenocrysts of diopside-augite ($Wo_{42}En_{42-43}$), biotite (^{IV}Al=2.45, $Mg^{\#}$70), and plagioclase (core $An_{81}Or_4$, periphery $An_{74-80}Or_{1-2}$), enclosed within a glassy matrix, containing plagioclase ($An_{56}Or_5$), ortho- and clinopyroxene, and Ti-magnetite microliths.

Bentonitized latite ash tuffs (the same as at the base of Stop 1), with separate lime concretions or thin lime layers, are exposed on the eastern scarp of the road. In character and stratigraphic position, the outcrop corresponds to the bentonite deposit Dobrovoletz (located eastward of Kardjali), that cannot be visited due to technical reasons. The bentonitized tuffs contain mainly ash-sized pumice clasts (Fig. 2-1), single adularized perlite, and dense latite clasts. Fragments of plagioclase are very scarce. Pumice is completely altered, and replaced mainly by clay minerals, calcite, and adularia (see Fig. 1-2). The clay fraction <2µ (Fig. 2-2) consists mostly of smectite, illite, and zeolite. A presence of about 10% illite layers in the smectite is estimated on the basis of the position of approximately 16° 2θ smectite reflection of the EG-solvated sample (according to the Table 8.3, Moore and Reynolds, 1997). Incomplete expanding of smectite after glycerol solution of previously Mg-saturated samples might be due to the presence of vermiculite layers. The structural formula of the clay is calculated on the basis of a formula unit of 11 oxygens (H_2O is not considered): $(Ca_{0.102}Na_{0.040}K_{0.197})$ $(Al_{1.107}Mg_{0.637}Fe^{3+}_{0.337}Ti_{0.019})$ $(Si_{3.887}Al_{0.113}O_{10})(OH)_2$ (average from 7 microprobe analyses). The lime concretions and layers contain also latitic fragments (with amphibole, biotite, and plagioclase microcrystals), and the same free crystals. Some layers are fine-grained mudstones of sedimentary or epiclastic origin, rich in calcareous fossils. They consist of smectite, calcite and tiny K-feldspar, plagioclase, quartz, and mica crystals.

It is supposed that clay minerals result from low-temperature alteration of fine ash or pumice of latite composition that takes place under slightly acidic conditions.

The afternoon route starts again from the town of Kardjali (Fig. B), as the way to Stop 1 is the same, and leaving behind the already visited deposit “Jelezni-Vrata”, our trip continues loking at the same zeolitized pyroclastics and their cover of mixed epiclastics (Fig. 1-1). The trachydacite volcano Hisar rises on the right. After the village of Jinzifovo, the

Table1.1 - Major elements content (%wt) of the zeolitized

Sample	1803	1804	1805	1806	1807
Location	1st flow	2nd flow	3rd flow	fall-out	4th flow
SiO_2	73.30	73.32	73.46	70.91	70.62
TiO_2	0.14	0.13	0.10	0.10	0.15
Al_2O_3	11.14	11.53	10.14	10.72	11.56
Fe_2O_3	1.38	1.19	0.41	0.84	1.55
MnO	0.01	0.00	0.01	0.04	0.01
MgO	0.39	0.32	0.25	0.40	0.40
CaO	1.31	1.20	1.20	1.51	1.63
Na_2O	1.85	1.45	0.79	1.64	2.13
K_2O	3.66	3.56	4.21	2.44	2.94
P_2O_5	0.12	0.08	0.09	0.07	0.11
H_2O	5.95	5.64	8.48	10.62	8.14
Somme	99.25	98.42	99.14	99.29	99.24

R-ray fluorescence analyses ("Eurotest", Sofia)

road crosses the Chiflik fault-flexure zone. The upright layers are fall-out tuffs (with clear ripple-marks), and thin ignimbrite deposits, similar to these seen at Stop 1. The mountain massif on the left is crowned by pale green zeolitized ignimbrites, and fall-out tuffs of the 1st acid phase (Stop 4); the epiclastics from the cover of Stop 1 are visible on the right. The trachyrhyodacite volcano Perperek (SiO_2=70.78-72, Na_2O=2.92-4.45, K_2O=4.53-6.62%wt) rises near the village of the same name, as the flat tops seen on the left are fan-like lava domes squeezed out from the vents of this volcano (Yanev et al., 1968). A repeated alternation (caused by fault displacements) of tuffs, epiclastics, and limestones, deposited during the 1st, 2nd and 3rd volcanic phases, can be observed going uphill above Perperek village. These products are covered by rhyolite conglomerate sandstones and clays, deposited in a river valley (called Paleo-Arda) more than 70 km long and 1-4 km wide, which developed at the end of the Oligocene volcanic activity. The Priabonian sediments appear again in the vicinity of the Miladinovo village. The subvertical pale green zeolitized ignimbrites of the 1st acid phase (the Lyaskovez mordenite deposit) are exposed in the area of the Lyaskovetz village. The products of the same volcanic phase are exposed uphill above the village, but here they are clinoptilolized, and displaced by normal faults. Afterwards the route crosses the eastern margin of the Silen volcano (SiO_2=75.13-76, Na_2O=3.5-3.6, K_2O=4.84-5.15%wt), which developed during the 4th volcanic phase. It lies on the Paleo-Arda alluvial deposits and is also associated with perlites. Then the road again crosses the deposits filling the Paleo-Arda valley (here E-W oriented), as well as the underlying tuffs of the 2nd acid volcanic phase, and the sediments, epiclastics, and latites of 2nd intermediate phase, within which Stop 3 is located.

Stop 3:

Perlite Deposit "Golobradovo"

Author: ***Y. Yanev (Geological Institute, Bulgarian Academy of Sciences).***

Table 1.2 - Mineral quantities (in %wt) of the zeolitized pyroclastics, Jelezni-Vrata deposit

Sample number and pyroclastic unite	Cl	CT	Ad +S	Sm	Il	Q	Pl	Mu	Others
1803 - 1st flow	42	12	17	1	8	16	3	-	lomontite gmelinite (?)
1804 – 2nd flow	38	15	14	1	10	16	3	2	
1805 – 3rd flow	54	13	6	2	5	15	1	3	
1806 – fall-out	57	10	1	9	6	11	5	-	gmelinite (?)
1807 – 4th flow	45	10	6	7	8	12	11	-	

Based on XRD, DTA and comparison of the whole-rock and mineral chemistry (analyzed by R. Pravchanska and P. Petrova, Geological Institute). Cl,clinoptilolite; CT, cristobalite-tridimite; Ad+S, adularia +sanidine; Sm, smecite; Il, Illite; Q, quartz; Pl, plagioclase; Mu, muscovite.

Volume n° 4 - from P14 to P36

Table1.3 - Chemistry of the zeolites (according Djourova and Alexiev, 1990)

Sample location	1st flow	3rd flow	Fall-out tuff
SiO_2	66.66	65.71	65.79
TiO_2	0.06	0.07	0.07
Al_2O_3	11.09	11.47	11.19
Fe_2O_3	0.33	0.45	0.49
MgO	0.48	0.43	0.51
CaO	2.10	2.22	2.83
Na_2O	2.47	1.41	0.80
K_2O	3.65	4.43	4.49
L.O.I.	12.76	13.54	13.68
Si/Al	5.10	4.84	4.98
Ca %	18	22	29
Na %	46	26	15
K %	36	52	56

Note: monomineral wet analyses

The stop is located 750 m awayand about 80-90 m uphill from the bus stop at Golobradovo village.

Introduction

The deposit of water-bearing volcanic glasses (perlites) is located 20-25 km to the east of Kardjali, and is connected with the Lower Oligocene volcano Studen-Kladenetz which belongs to 2nd acid volcanic phase. The K-Ar age of the trachyrhyolites and perlites of the Cholderen Summit is 32-33 Ma (Lilov et al., 1987; Georgiev et al., 2003). The perlites were found and firstly described by Goranov et al. (1960). A twofold trench and drill-hole exploration of several perlite deposits associated with this volcano was performed during the 1970s and at the beginning of the 1980s. Because of the relatively high density of the expanded perlite and its high Fe content, these deposits have not been exploited.

Application

Natural perlites are mainly used (after preliminary heating at 300-350°C) for expanded perlite production by fast heating at 1200-1300°C. Practically, the expanded perlite is an artificial pumice material, having a relative weight from 60 up to 500 kg/m^3 (according to the type of the products), with good fireproofing, as well as heat and sound insulating properties (0.04kcal/mh°C). The expanded perlite is used mainly as a light filler of prefabricated building elements, and the waste (40% resulting from the production) represents the fraction <2.5 mm – in the glass and ceramic industries.

Geology of the Studen-Kladenetz volcano

(Fig. 3-1). The volcano is elongated in an E-W direction, and is composed of several large domes, with a complex structure (up to 3x1 km in size), and producing hyaloclastic flows (up to 1 km long), numerous smaller domes (having diameters from

Figure 2-1 - Bentonitized tuffs; (1) pumice clast. // N. The bar is 0.25 cm.

tens, to several hundreds of meters), and sills. All these bodies are emplaced on an area of about 20 km^2, i.e. the volcano morphology is transitional between that of a dome volcano and a dome-cluster (Yanev, 1998). The volcano basement is built of sediments, latite pyro- and epiclastics, as well as of the frontal parts of two latite sheets from the northern foot of the St. Ilia volcano (2nd intermediate phase), located to the south of the Studen-Kladenetz volcano. The body of the volcano interfingers with the explosive

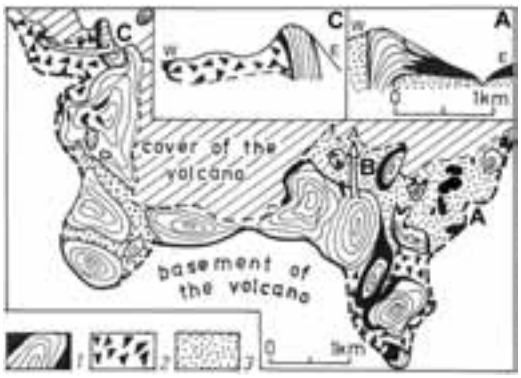

Figure 3.1 - Geological sketch map of Studen-Kladenetz volcano (Yanev, 1987): (A) Golobradovo (Stop 3), (B) Svetoslav and (C) Konevo perlite deposits. In the corner: schematic cross sections of (A) and (C). Key: (1) trachyrhyolite dome with perlite periphery, (2) perlite breccia, (3) acid tuffs and latite-trachyrhyolite epiclastics; white arrows indicate the hyaloclastic flows.

products of the 2nd acid phase, having a thickness of 50-70 m (these latter being pumice and perlite tuffs, corresponding to the zeolitized tuffs of Jelezni-Vrata deposit – Stop 1), with epiclastics (70 m thick), and with the overlaying
limestones (130 m thick). The epiclastics are of acid composition, silty, sandy to granule. Only in the central and western parts of the volcano are they of mixed composition (containing rounded perlite, trachyrhyolite, latite, and gneiss clasts up to 20-30 cm in size, and enclosed by an ash-pumice matrix), poorly-sorted to chaotic. The domes are emplaced at different levels: only in the volcano basement (in the central parts), in tuffs and mixed epiclastics, and in the limestones (in the central and western parts).

The volcanic domes have a zonal structure: a core built up of red flow-banded trachyrhyolites, and a periphery – of black to gray perlites. The later form lens-, sickle-, or ring-like bodies. The trachyrhyolite/ perlite transition could be of two types (Yanev, 1987): 1) alternation of trachyrhyolite and perlite layers or

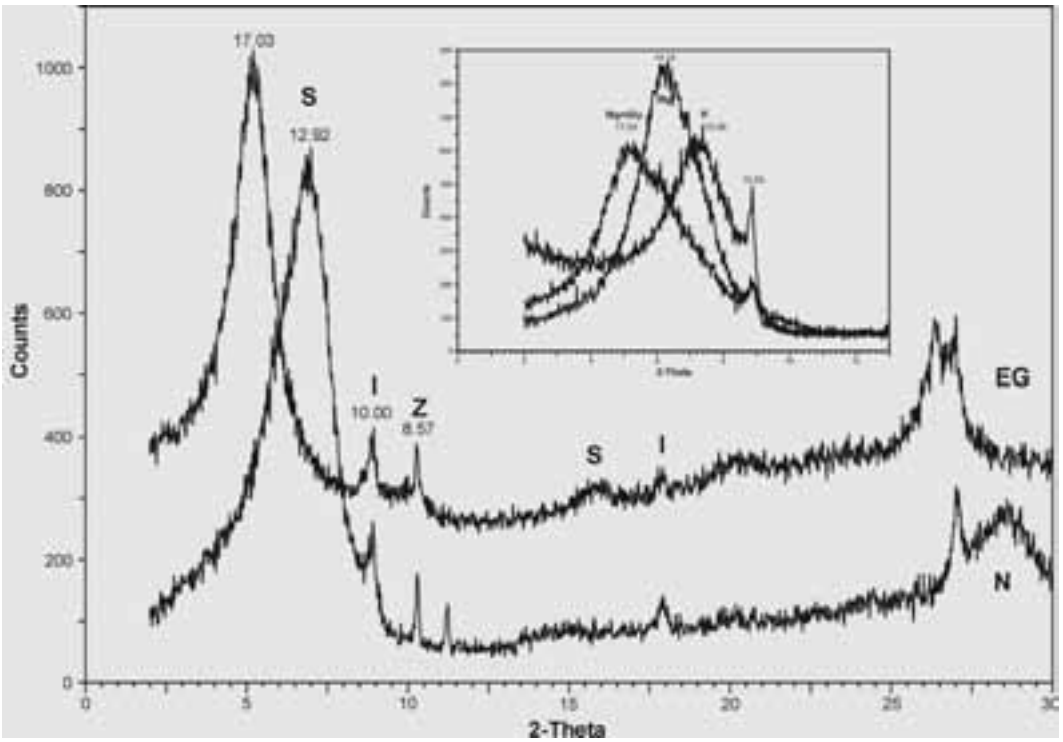

Figure 2.2 - XRD-patterns of the oriented clay fraction of the bentonitized latite ash tuff after different treatments. N – air-dried, EG – ethylene glycol saturation. Inset: Mg+Gly – first Mg-, then glycerol saturation K – K saturation; d-values in Å. S – smectite, I – illite, Z – zeolite.

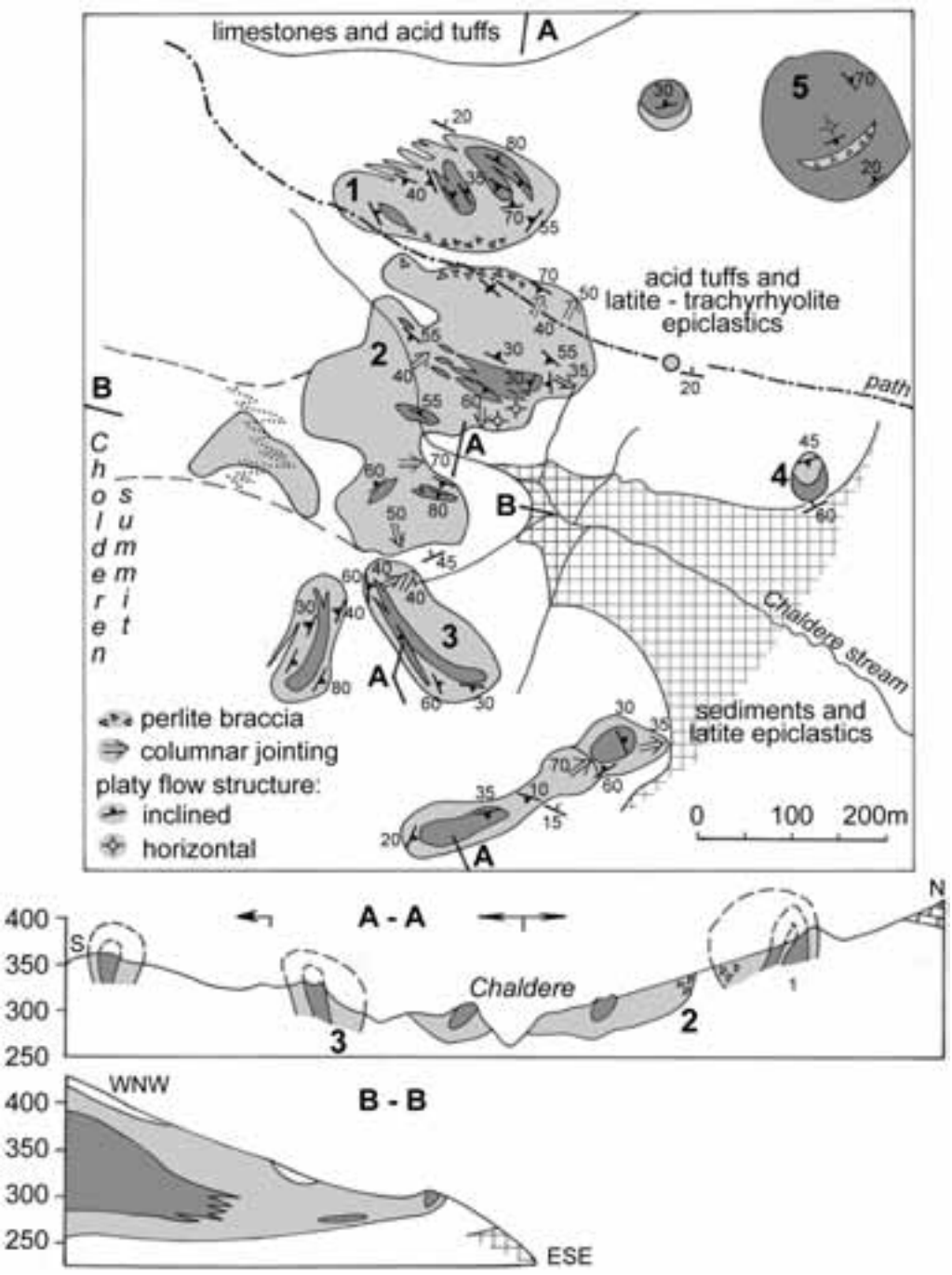

Figure 3.2 - Geological map of the Golobradovo perlite deposit (Stop 3) (mapped by Yanev in 1975 on scale 1:10 000). The gray area is perlite and the black one is trachyrhyolite. Key: (1) Odjak-Kaya dome, (2) sill (dashed line - not exposed part of the sill and dotted line – schematic position of the perlite/trachyrhyolite transition zone), (3) Central dome, (4) Small dome and (5) North-eastern dome. A-A and B-B – cross sections shown at the bottom.

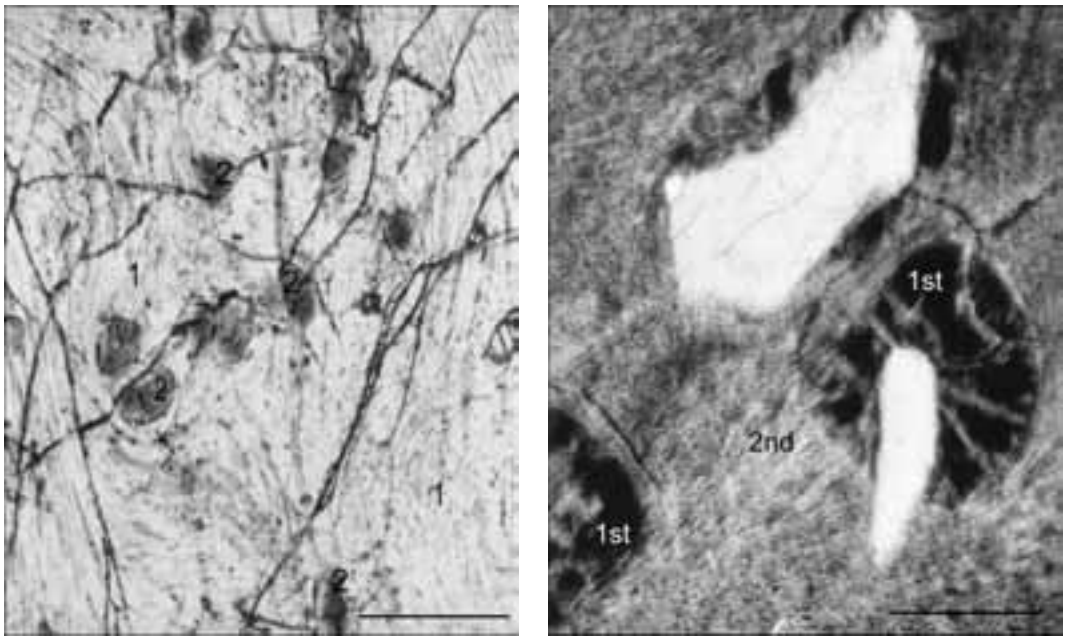

Figure 3.3 - Microphotographies of the Golobradovo deposit: left, deformation of the Fe-oxide microlithe flow bands in the glassy matrix (1) by the trahyrhyolitic spheruloids (2) (the bar is 0.25cm); right, two generations spherolites (1st and 2nd) in trachyrhyolite spheruloid with diameter 10cm (perlite / trachyrhyolite transition zone (the bar is 0.25 cm). // N.

lenses; 2) areas of trachyrhyolite spheres, enclosed by a perlite matrix. In the first case, the layers are up to 10-15 cm thick, as the thickness of trachyrhyolite layers gradually decrease (to a few mm), towards the perlite periphery, and finally disappear. Alternatively, the perlite layers thin towards the trachyrhyolite core. Along their strike. the trachyrhyolite layers (as well as the perlitic) grade into wedges and disappear i.e. the two rock varieties interfinger laterally with one another. The trachyrhyolite spheres (spheruloids - Yanev, 1970), in the second type of transition, are up to 10-15 cm in diameter, and have a spherolitic texture.

At the perlite periphery, the spheruloids gradually decrease in number, and finally, they also disappear.

In the Golobradovo deposit, the trachyrhyolite/perlite transition is mostly a combination of these two types: lineally-arranged trachyrhyolite spheruloids, stuck onto trahyrhyolite layers. Vesicles (from several mm up to 10-15 cm in size), are observed only in the trachyrhyolite spheruloids and layers. Some of them are partly-filled with opal-chalcedony aggregates.

There are three hypotheses on the genesis of the trachyrhyolite layers and spheruloids (Yanev, 2000):

• products of suppressed crystallization, due to the fast increase of the cooling rate towards the dome periphery,

• products of the partial crystallization of parts of already litified glass (devitrification),

• products of subliquidus immiscibility, in which the super-cooled water-containing lava (the presence of water in acid lavas has been proved by Hervig et al., 1989) splits into two immiscible liquids. One of them is rich in water, and after cooling, produces perlites; the other dry melt crystallizes, and generates trachyrhyolite layers or spheruloids. Available petrologic data are in agreement with this hypothesis (see below).

Dome-connected flows consist of gray hyaloclastic (Svetoslav and Konevo deposits). Their emplacement in an marine environment is marked by the coral reefs grown on them. Tens of meters in size trachyrhyolite bodies, enclosed by the above-described transition zones, are also present within the flows. The hyaloclastic flows grade into massive perlites towards the necks, as the trachyrhyolite/perlite transition is an alteration of layers (Konevo deposit), or an interfingering between perlite and trachyrhyolite wedges (Svetoslav deposit). The sill (made up of Golobradovo deposit), consists of black massive

Volume n° 4 - from P14 to P36

perlites, and also contains trachyrhyolite bodies. In previous works, it has been described as perlite flow (Yanev, 1987, Popov et al., 1989)

Geology of the Golobradovo deposit

(Fig. 3-2). This deposit is located in the eastern periphery of the Studen-Kladenetz volcano. The deposit includes a dozen small domes (the larger three ones are 240x150, 220x80 and 160x60 m in size), having black to dark gray perlite peripheries (trachyrhyolite/perlite ratio is 1:5 to 1:4), as well as one neck-connected thick sill. ***The domes*** intrude the sedimentary, epi- and pyroclastic rock from the volcano basement, about 50-60 m below volcano bottom, i.e. they cooled at shallow subvolcanic level as cryptodomes. Dome-rounding colluvial breccias, typical of subaerially erupted domes are absent. The perlites exhibit columnar jointing, with hexagonal or pentagonal columns (20-25 cm in diameter) perpendicular to the cooling surfaces, i.e. most often horizontal. At the contact with perlites, the hosting tuffs are silificied and zeolitized (platy clinoptilolite crystals within a chalcedony matrix), and have a glass-like appearance. The shape of ***the sill*** is L-shaped in planar view. It is probably connected to a neck located 200 m to the WNW of the sill outcrop (Cholderen Summit). Close to the neck, the perlite interfingers with trachyrhyolites. Here, the sill is 150 m wide at a thickness of about 20-30 m, and includes two large "lenses" (tens of meters in size) of hosting sedimentary and epiclastic rocks. The eastern outcropping part of the sill is elongated in a SW-NE direction, and is 350x200 m in size (the thickness varies from 80 to 25 m) i.e. this is the largest perlite body in the deposit. It is almost entirely exposed on both banks of the Chaldere stream. The perlites exhibit columnar jointing (column diameter is 12-20 cm) or are brecciated in the lob of the sill. Due to the uneven sill bottom, the columns are often not vertical, but angled (along the Chaldere stream). The internal structure of the sill is complicated by the presence of numerous small trachyrhyolite "lenses" (especially in its lower parts), and two subvertical bodies 20x50 and 40x130 m in size, displaying combined perlite/ trachyrhyolite transition (spheruloids "grown" on trachyrhyolite layers). The trachyrhyolites show clear flow banding and parallel jointing.

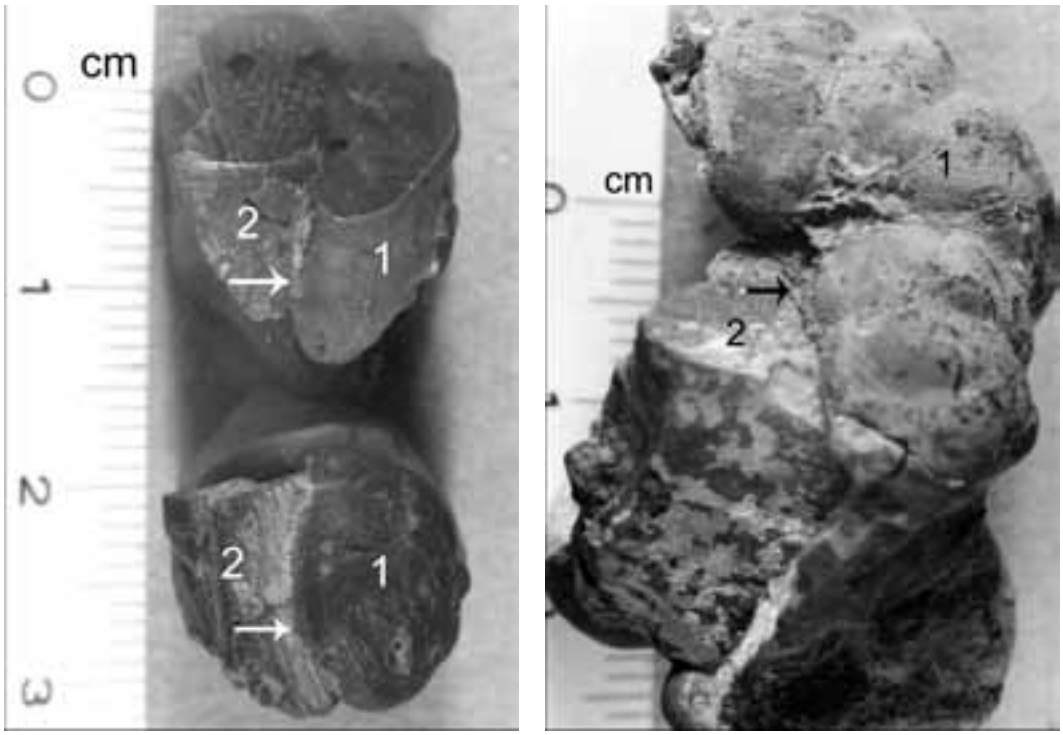

Figure 3.4 - Trachyrhyolite spheruloids (1) with menisci (arrows) located on the trachyrhyolite "layer"; (2) in the perlite / trachyrhyolite transition zone (Small dome). The perlite matrix is eroded.

Petrographic characteristics

The perlites consist of phenocrysts up to 1-2 mm in size and matrix. The phenocrysts are of sanidine ($Or_{59.4-66}Ab_{33-40}$), plagioclase (An_{22-25}-Or_{6-7}), biotite ($Mg^{\#}$31-38, ^{IV}Al 2.46-2.55 with 0.3% F), less augite ($Wo_{40}En_{23-25}$), and microphenocrysts of quartz (Yanev, 1998); the accessory minerals are magnetite, apatite, and zircon. The magma temperature, calculated using the two-feldspar geothermometer of Fuhrman and Lindsley (1988), is 776°C. The matrix is of dark volcanic glass with perlitic cracks, and numerous, mainly feldspar microlites, and dendrite-like crystallites. They are arranged in bands curving around the phenocrysts and spheruloids (Fig. 3-3, left), which is one of the indicators of their origin from immiscible liquids (Roedder, 1979). The spheruloids have a spherolitic texture, and often enclose (Yanev, 1970, 2000) an earlier generation of spherolites (Fig. 3-32, right). The spheruloids that lay on the trachyrhyolite layers have menisci (Fig. 3-4), that is "unequivocal evidence for immiscibility" (Hanski, 1993).

The trachyrhyolites contain the same phenocrysts as perlites, but their matrix is of felsitic or locally axiolitic texture, consisting of feldspar and tridimite microcrystals (Dimitrov et al., 1984). Their colour is red (at a depth of several tens of meters – gray), caused by the superficial oxidation of microlithic magnetite dispersed in the matrix. Some of the spheruloids which contain latitic enclaves having diffuse outlines, and are composed of a glassy matrix with microlithic plagioclase and pyroxene, indicating a process of magma-mixing (Yanev, 1998).

Chemical composition

Both perlites and trachyrhyolites are rich in alkalies (Table 3-1), and an obtained K/Na ratio of 1.5 is typical of most Eastern Rhodopes acid volcanics (Yanev et al., 1983). The normative composition of perlite is: quartz 29%, K-feldspar 44%, and albite 27% (Yanev and Zotov, 1995). Compared with trachyrhyolites (water free base, Table 3-1), perlites have a lower content of SiO_2, higher K, and lower Na contents, and, relatively, a much higher K/Na ratio. Since Na cation hydrates easily compared with K, due to its smaller size and is relatively leached to a greater degree, the lower Na contents are widely considered as evidence supporting the hypothesis of a later perlite hydration (Noble, 1967; Steward, 1979). However, in the Eastern Rhodopes, in perlites, the correlation between water content and K/Na ratio is negative (Yanev, 1987, 1994).

The alkali contents in transitional zones change gradually from the trachyrhyolite core to the perlite periphery (Fig. 3-5): in the trachyrhyolite layers, Na, K, and Rb decrease gradually, in perlite ones, Na increases, K does not changes significantly, and Rb decreases. Thus, Na and Rb contents in the perlite periphery and trachyrhyolite layers become equal. The additional hydration cannot explain these gradual changes, which most probably are due to the immiscibility (Marakushev and Yakovleva, 1980; Yanev, 2000). The earlierly generated smaller spheres in the spheruloids (Fig. 3-3) have almost equal contents of Na and K (Na_2O=4.35, K_2O=4.69%wt), while the hosting larger spheres (2nd generation), show the significant predominance of K (Na_2O=3.39,

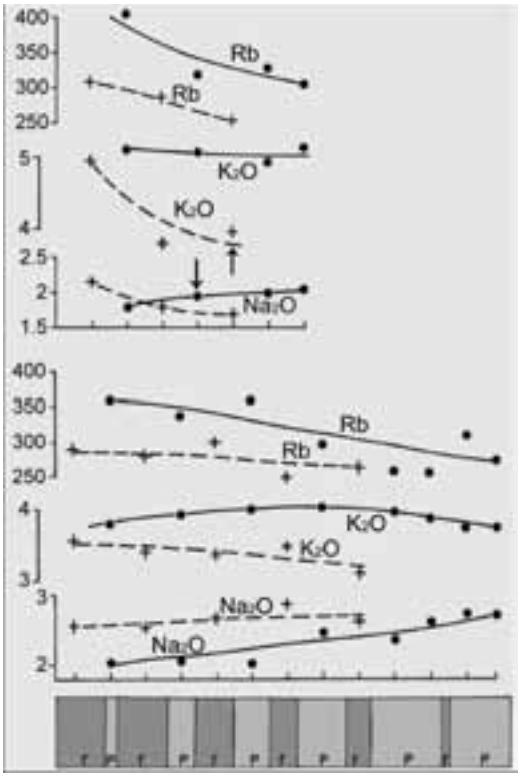

Figure 3.5 - Na_2O, K_2O (%wt) and Rb (ppm) contents (flame photometry, analyzed by B. Karadjova) of the perlite (solid circles and solid lines) and trachyrhyolite (crosses and dashed lines) layers in the transition zone along two profiles across the Central dome periphery (left, to the trachyrhyolite core, right, to the perlite periphery). Bottom, schematic cross section of the perlite, trachyrhyolite transition (p, perlite and r, trachy-rhyolite). The arrows indicate the trace element analyzed samples (Table 3-2).

Volume n° 4 - from P14 to P36

K_2O=6.62%wt, Yanev, 1970), which also can be explained by occurrence of immiscibility, but in two stages (Yanev, 2000).

The contents of almost all trace elements (Table 3-2) in the perlite layers from the transitional zone, are higher than these in the trachyrhyolite layers, especially of Ti, Mn, Cs, and Rb, because of their crystallochemical properties regarding the glass formation (Yanev, 1994, and references therein) i.e. Ti^{4+} is a glass-forming cation; Cs^{+}, Rb^{+}, as well as Mn^{2+}, $Zn^{2+,}$ and Pb^{2+} are modifier cations in the glass texture because of the favorable metal-oxygen bonds they form. The only trace element prevailing in the trachyrhyolites is Li, cation-stimulating crystallization of the alumo-sillicate melts.

Perlite nanostructure

X-ray- and spectroscopic methods allow a view on the nanostructure of the volcanic glasses, which like the synthetic alkali alumo-silicate glasses, show only short-range order (i.e. up to 2-3 neighboring ions, or up to a distance of about 8 Å, respectively), and are disordered in medium- and long-range order. Using X-ray radial distribution function analysis (Zotov et al., 1989), the following distances between network forming ions, arranged in 6-membered rings, have been measured (in Å): Si,Al-O_1=1.62, O-O_1=2.68, Si,Al-Si,Al_1= 3.15, Si,Al-O_2=4.12, Si,Al-Si,Al_2, and O-O_2=5.265, and the angle is 153°. The nanostructure of the Golobradovo perlite is similar to that of the feldspar glasses (Taylor and Brown, 1979), but the Si,Al-O-Si,Al angle in volcanic glasses is 10° larger, due to the tetrahedral rings expansion that might have resulted from presence of water molecules (Zotov et al., 1989).

A special modifier cation is Fe, as its valence state defines the perlite color and, consequently, the possibilities for its use in the glass industry. It was found by EPR spectroscopy (Calas et al., 1988), that the Golobradovo perlites contain Fe^{3+}, mainly in nanocrystals (signal at g=3.2), and much less as ions in the glass structure (signal at g=4.3). Mösbauer measurements (Dormann et al., 1989) performed at room temperature, 77° and 4.2°K (Fig. 3-6), show the following distribution of Fe in the Golobradovo perlites: magnetite microliths (>30 nm in size) – 32%, hematite nanoaggregates (15-30 nm) – 17%, wustite nanoagreggates (<15 nm) – 25%, Fe^{2+} and Fe^{3+} in the glass structure – 17 and 9%, respectively. The presence of FeO nanoaggregates in the glass structure is indicative of the reduction conditions at T_g point, e.g. during the perlite cooling. The high contents of black nano- and microcrystals, the high ratio mineral phases/structural Fe (2.85), and total high Fe contents in perlite (1.65 wt%), define its black color. The presence of Fe^{2+} ions in the glass structure is responsible for its bluish shade. Thus, the perlite coloring is of colloid type (the colored compounds have colloid size – Kocik et al., 1983). The gray perlites contain less black nano- and microcrystals, and the main part of the Fe is as cations bonded to the glass structure.

The water present in perlites is the main cause for their expanding. It is known (Scholze, 1959) that water in glasses exists as molecular water and hydroxyl groups bonded to the glass structure. Infrared studies of the Golobradovo perlites showed the presence of OH-groups and two groups of molecular water (Dimitrov et al., 1984; Yanev and Zotov, 1996, and references therein). The perlite spectrum is characterized by bands at 3588, 3233 cm^{-1} (combined bands of two groups molecular water), and 3450 cm^{-1} (band of the OH-groups); and in NIR (Fig. 3-7) - 5260 and 5155-5025 cm^{-1} (of the molecular water) and 4535 cm^{-1} (of the OH-groups), respectively. The absorption band position in the 3000-3600 cm^{-1} interval has revealed (Yanev and Zotov, 1996) the average hydrogen bond distance R (O...O) of the OH groups in the volcanic glasses to be about 2.9 Å, and those of the molecular water, 2.8 Å (ice type H-bond) and 3.1 Å. The distances O-H of all water species are 0.94-0.97Å.

The TGA-curves (Fig. 3-8, Bagdassarov et al., 1999) show that the most significant molecular water evaporation occurs at 320°C, and the total water loss takes place at about 600°C. Above this temperature, only structurally-bonded OH-groups remain in the glass. It is supposed that during dehydration, a part of the molecular water dissociates, and additional OH-groups enter the glass structure. The OH-groups do not escape totally, even during heating at temperatures corresponding to the perlite expansion (e.g. about 1200-1300°C, Fig. 3-7). Hence, the expansion of perlite results from rapid evaporation of the little H_2O remaining (after 300-350°C preheating of the perlite), as well as of a part of OH-groups from the softened glass (having viscosity of 10^8-10^7 Pa) heated above T_g (Bagdassarov and Dingwill, 1994).

Technical characteristics. Expanded perlites obtained from the Golobradovo deposit have a high density (144 kg/m^3 of 0.2-2.5 mm fraction). Despite this, they can be used as a filler in concrete, as a 2.5-

Table 3.1- Major elements content (%wt) in the trachyrhyolites and perlites from the Golobradovo deposit, Studen-Kladenetz volcano

Volcanic body	Odjak-kaya dome (1)	Perlite sill (2)				Central dome (3)				Little dome (4)	NE dome(5)
Rock variety	perlite	perlite	perlite	trachy-rhyolite	perlite	trachy-rhyolite	perlite	trachy-rhyolite	perlite	trachy-rhyolite	trachy-rhyolite
Position in the dome	periphery	periphery	periphery	transition zone		core	periphery	transition zone		Core	
Analysis nº	average	1165	G-73	769	768	SK-337	SK-796	794	793	SK-325	SK-327
SiO_2	69.03	71.07	70.14	74.70	70.13	74.73	70.33	75.30	69.75	74.47	74.18
TiO_2	0.11	0.14	0.14	0.12	0.13	0.13	0.14	0.12	0.15	0.11	0.11
Al_2O_3	13.30	13.04	13.49	12.88	13.06	11.78	12.89	11.37	13.13	12.24	12.50
Fe_2O_3	1.75tot	1.67tot	1.15	0.76	1.23	1.03	2.00tot	0.75	1.01	0.94	1.03
FeO			0.50	0.72	1.08	0.36		0.58	0.90	0.86	0.46
MgO	0.30	n.d.	0.23	0.80	0.30	0.15	n.d.	0.05	0.06	0.27	0.25
CaO	1.12	0.72	0.60	0.52	0.61	1.08	0.74	1.32	0.93	0.96	0.46
Na_2O	3.09	3.40	2.86	3.64	2.80	3.60	3.06	2.45	2.74	3.60	3.70
K_2O	5.12	5.69	6.62	5.46	6.10	5.21	5.88	4.50	6.00	5.10	5.30
P_2O_5	n.d.	n.d.	0.03	0.01	0.03	0.02	n.d.	0.01	0.01	0.03	0.02
H_2O^- (105ºC)	1.20		0.40	0.26	0.45	0.55		1.64	0.88	0.50	0.39
H_2O^+ (1050ºC)	5.18	4.2tot	3.60	0.07	3.64	0.84	4.45tot	2.18	4.11	0.63	0.57
Total	100.20	99.93	99.76	99.94	99.56	99.48	99.49	100.27	99.67	99.71	98.97
Water fry base											
SiO_2	73.58	74.25	73.24	75.01	73.46	76.19	74.00	78.07	73.67	75.56	75.68
TiO_2	0.12	0.15	0.15	0.12	0.14	0.13	0.15	0.12	0.16	0.11	0.11
Al_2O_3	14.18	13.62	14.09	12.93	13.68	12.01	13.56	11.79	13.87	12.42	12.75
Fe_2O_3	1.86tot	1.74tot	1.20	0.76	1.29	1.05	2.10tot	0.78	1.07	0.95	1.05
FeO			0.52	0.72	1.13	0.37		0.60	0.95	0.87	0.47
MgO	0.32	n.d.	0.24	0.80	0.31	0.15	n.d.	0.05	0.06	0.27	0.26
CaO	1.19	0.75	0.63	0.52	0.64	1.10	0.78	1.37	0.98	0.97	0.47
Na_2O	3.29	3.55	2.99	3.65	2.93	3.67	3.22	2.54	2.89	3.65	3.78
K_2O	5.46	5.94	6.91	5.48	6.39	5.31	6.19	4.67	6.34	5.17	5.41
P_2O_5	n.d.	n.d.	0.03	0.01	0.03	0.02	n.d.	0.01	0.01	0.03	0.02
K_2O/Na_2O	1.66	1.67	2.31	1.50	2.18	1.45	1.92	1.84	2.19	1.42	1.43

Note: wet chemistry analyses (analyses with Fe_2O_3 and FeO) and R-ray fluorescence (analyses with total Fe as Fe_2O_3tot)

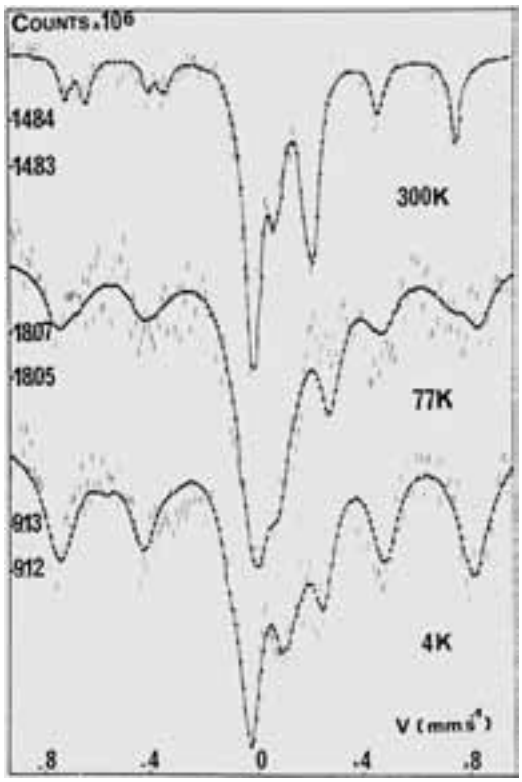

Figure 3.6 - Mössbauer spectra of Golobradovo perlite (sample G 73) at three different temperatures (in °K) according to Dormann et al. (1989).

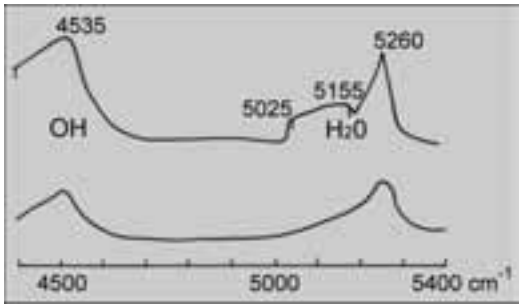

Figure 3.7 - Near infra-red spectra of Golobradovo perlite (sample G73) before (top, according to Yanev and Zotov (1996) and after expanding at 1300°C (bottom).

5.0 mm fraction has a high compressive strength: 16.8 MPa and density of 490 kg/m^3 at 30 sec expanding, or 27.0 MPa and 470 kg/m^3 at 60 sec expanding (Popov et al., 1989). For comparison, the perlite breccia (for example, of the Svetoslav deposit) gives expanded perlites with a lower density - 102 kg/m^3.

From Stop 3, we go back by the same road to the Chiflik village (Fig. B), from where we continue to travel to the NE in the Priabonian flysch deposits outcropped along the valley of the Perperek River. Both slopes are crowned by zeolitized pyroclastics of the 1st acid phase, in which Stop 4 is located.

Table 3.2 - Trace element contents (in ppm) of perlite and trachyrhyolite (Golobradovo deposit)

Analyses n°	**793**	**794**
Rock variety	perlite	trachyrhyolite
Li	2.65	3.66
Rb	235	107
Cs	29.25	7.75
Sr	49	32
Ba	74	>70
Zr	234	201
Ti	845	714
Mn	507	181
Pb	38	32
Zn	34	25
Cu	8	11
Ni	35	19
La	70.8	64.0
Ce	155	131
Sm	8.4	7.7
Eu	0.30	0.30
Tb	1.22	1.03
Yb	5.8	4.8
Lu	0.85	0.70
Th	62.2	49.5
U	11.5	9.8
Sc	4.1	3.4
Hf	6.3	5.2
Co	0.7	0.7
V	0.5	0.5
Ta	5.8	4.2
Nb	18.4	18.2

Li, Pb, Zn, Cu, Ni - atomic absorbtion; Rb, Sr, Ba, Zr, Ti, Mn – R-ray fluorescence; REE, Cs, Th, U, Sc, Hf, Co, V, Ta - NNA; Nb -colorimetry

Stop 4:

(facultative) – Thrace holly HILL (from 18th century B.P. to 14th century A.D.): Castle and sanctuary, cut in the zeolitized pyroclastics. Byzantine castle "PERPERICON"

Geological remarks (author Y. Yanev).

The holy hill, which represents an archeological site, is built up by low-to medium-grade fine-grained pumice ignimbrites, deposited from the pyroclastic flows of the 1st acid phase. The supposed vent area of these volcanics (Yanev and Bardintzeff, 1996), is located about 15 km to the west of Stop 4, in the region of the village of Kostino (Fig. B). The pyroclastics are zeolitized, and are perfect building stone, having been completely preserved for as long as 25 centuries. The enormous zeolite deposits of Gorna-Krepost and Most are located in front of the hill on the NE slope of the river, where the same pyroclastics are also zeolitized. The average mineral composition (calculated on the basis of 101 and 120 samples of both deposits) is: 84% and 78% clinoptilolite, 4.5% and 5.3% montmorillonite, 1.4% and 2.5% celadonite and illite (giving the pale green color of the rocks), 1.9% and 2.5% opal-CT, 0.2% and 0.6% calcite, 7.5% and 6.4% cristallo- and lithoclasts; C.E.C (measured in 5 samples) is 100-133 and 80-128 meq/100g, for Gorna-Krepost (Raynov et al., 1997). The thickness of the zeolitized pyroclastics there reaches 110 m.

Historical remarks (according to web-site **www.perperikon.bg**). The earliest traces of human civilization discovered so far at Perperikon were dated to the late Neolithic Period, 6th-5th millennium BC, but the earliest pits hewn in the rock were dated to the late 5th - early 4th millennium BC. During the late Bronze Age, in particular, 18th-12th century BC, and later during the early Iron Age (11th-6th century BC), Perperikon saw its first heydays as a Trachian cult center, as the first period probably coincided with the peak of the Mycenaean and Minoan civilizations. At that time, a citadel (Acropolis) was built, whose stone walls are 2.8 m thick and which surround numerous temples and civil buildings with monumental portals (the ground floors are entirely carved in the rocks). A giant palace, being also a temple of Dionysus (it is known that Thracian rulers possessed both secular and religious authority), enclosed by 2.5-2.6 m thick stone walls, is attached to the citadel. 50 chambers, having an area of 17 000 m^2, built on seven levels, across a gradient of approximately 30 m, are identified. A huge oval hall, apparently left roofless, was discovered in the palace. At the center of this open space, a magnificent round altar was sculpted from the rock (2 m in diameter, and rising 3 m above the floor level). At least two oracles of momentous significance for human history can be connected with this altar. When Octavian, father of Augustus, came upon the Holy Mount of Dionysus, he consulted the oracle about his son, and the Thracian prophets said to him that his son was to rule the world, for, as the wine was spilt onto the altar, the smoke rose up above the top of the shrine and even into the heavens, as had happened when Alexander the Great himself had sacrificed upon that same altar. Wine and fire were used to deliver the prophecy: wine was spilt onto the altar and the height of its flame signified the prophetic

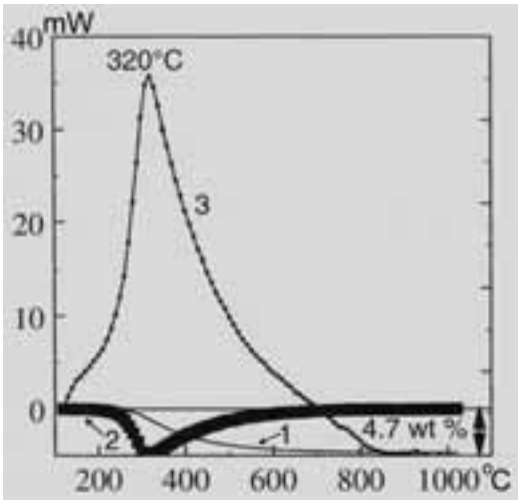

Figure 3.8 - Results of TGA (1, in wt%), DTG (2, in 0,1mg/min) and DSC (3, in mW) of Golobradovo perlite (sample G73) obtained in a thermal gravitational balance with heating rate of 5 K/min (according to Bagdassarov et al., 1999).

answer. A throne hall, 30 m long, with massive throne carved out in the tuffs, and a sewer system draining the rainwater into two large cisterns (12/5/6 m), have also been found in the palace. Many basins on two levels, carved in the rocks, are found around the hill, probably used as winepresses ("sharapani").

This cult center was revived and enhanced after Thrace was conquered by the Romans (in 45 AD). During the 4th century, Perperikon was captured and burned by the Goths, but in the 5th century, the city became a center of Christianity. Later, the main city

of the Byzantine province of Achridos was located at the foot of Perperikon, which was the seat of the regional governor of Achridos and also as episcopal center, with large monastery complex and necropolis (a cruciform pendant reliquary, containing pieces of wood, believed to be fragments of the True Cross, was found in one of the grave chambers). The town had significant importance during the 11th-14th centuries. It is supposed that the gold used for the coins of 21 1/3 carats, struck by the Byzantine Emperor Alexius I Comnenus in 1082 AD, and called "hyperpyron" (it is thought that the name is connected to the melting and refining of gold by fire) came from the gold mine, located just few km away (within the silicified Priabonian sediments). Later the coin was named "perpera", and that might be the source of the names of the citadel ("Perperikon") and of the nearby river – Perperek. At the end of the 14th century, the town was conquered by Ottoman Turks, but up to the 17th century, the settlements near Perperikon remained Christian.

After Stop 4, our route crosses the same Priabonian sediments, which at the village of Stremtsi are cut and interbedded by latites erupted by one strongly-eroded Priabonian volcano. Its central parts are crossed by a NW-SE trending graben, where zeolitized pyroclastics of the 1st acid phase are exposed, and where three large zeolite deposits located. From north to south, these are Beli-Plast, Gorna-Krepost and Most. At the ridge to the north of the Perperek River, along the road, several-meters high rock "mushrooms" are formed within the zeolitized pyroclastics of the 2nd phase (the upper part of the "mushrooms" is the coarse-grained base of a pyroclastic flow). The quarry for obtaining 70 m thick zeolitized fall-out tuffs (Beli-Plast deposit) is near here. The average mineral composition (calculated on the base of 56 samples) of the zeolitized pyroclastics is: 80% clinoptilolite, 6.2% monmorillonite, 2.9% illite and celadonite, 1% opal-CT, 0.6% calcite, 10.5% crystallo- and lithoclasts; CEC (measured in 5 samples) vary from 90 to 150 meq/100g (Raynov et al., 1997). The Priabonian sediments outcrop along the road up to the town of Haskovo, where we enter the Neogene Thracian depression and the route back to Sofia is the same as the day before.

SECOND PART: Milos Island

General Information

Milos has been a well-known island since ancient times, due to its location and history. Most probably its name comes from the ancient hero "Milos". The island became more famous after 1820, when the statue of "Venus" was found and then transferred to the museum of the Louvre, in Paris.

The first known settlement of the island was "*Philakopi*", which thrived in the period from the 4th millenium till 800 B.C.. Milos at that time had established a well-developed commercial activity, exporting mainly tools and weapons made of obsidian. After Philakopi declined, the Dorian town of "*Klima*" was founded. Klima is located at the mouth of Milos bay. It was destroyed during the Peloponnesian War (431-404 B.C.), was later rebuilt under the Spartan domination, and endured the tribulations of the Roman and Byzantine times. Traces of Franks, Venetians, Turks, and even pirates, are evident in the island today.

The capital and port of Milos is "Adamas". The most interesting sights of the town are the churches of Aghia Triada (13th century) and Aghios Charalambos, with remarkable post-Byzantine icons and very old hand-carved wooden temples. The Museum of Mining and Geological Interest is also in operation in Adamas, giving important information about the quarry activities on the island and exhibiting a rich mineralogical collection.

"Plaka", the old capital of Milos is built on a rather flat lava flow. Its architecture is typically Cycladic. The ruins of a Frankish castle are visible on top of the hill, while a beautiful view is available for those who manage the 30-minute climb, and visit the church of "Korphiatissa". Inside the castle, there is the church of "Thalassítra", which was built in the 13th century. In Plaka there is also an archaeological museum with a lot of finds from various historic and prehistoric periods of Mílos. The Folklore Museum has a collection of folk artifacts, samples of the island's minerals, photographs, and historical documents of the greatest interest.

Near the town, the visitor can see the wonderful Roman mosaics (near a place called "Tramithia"), the Roman walls, the theatre and the baptistery. Nearby, there is the village "Tripití", with the famous catacombs that date back to the beginning of the Christian era.

"Pollonia", a picturesque former fishing village, is built on the northeastern part of the island, near which the ruins of the ancient town of Flakopí are located.

Regional Geologic Setting

Author: M. Fytikas (Aristotle University of Thessaloniki, School of Geology)

Introduction

The volcanic island of Milos is situated in the SW part of the Cyclades Islands group, and is a relatively small but significant portion in the central part of the South Aegean Active Volcanic Arc (SAAVA).

The SAAVA extends from the Greek mainland in the west, through the islands of the Dodecanese in the east (Fig. 1). It was formed during the Pliocene-Quaternary, as a consequence of the northward subduction of the African Plate beneath the Aegean microplate, and is still active (Fytikas, 1977; Fytikas et al., 1986; Markopoulos & Katerinopoulos, 1986). The Arc is no more than 20km wide, and its *outer part* extends from Crommyonia, through Methana, Aegina, Poros, Milos, Santorini, to Nisyros and western Kos (Fytikas et al., 1984).

Volcanism occurred concurrently along the arc (Fytikas et al., 1976; Innocenti et al., 1979; Fytikas et al., 1984), beginning at the end of the Early Pliocene (4,5 Ma), and continuing up to today (McKenzie, 1978; Mercier 1989; Pe-Piper et al, 1983; Fytikas et al., 1984).

Milos is almost totally built up of volcanic rocks. Outcrops of the pre-volcanic units are observed in the southern part of the island, and consist of a crystalline basement and of a neogene sedimentary formation (Fig. 2).

The metamorphic basement of Alpine age belongs to the South Cyclades Unit, and consists of re-crystallized metasediments, such as clay stones, sandstones and limestones, mainly under greenschist facies conditions (Durr et al., 1978). Blue-schist facies also were identified. Fragments of metamorphic rocks occur often as xenoliths in phreatic eruption, and more rarely in pyroclastic products.

Geological Evolution

During the subduction in the Tertiary, Milos Island was submerged. This procedure lasted until the Early Oligocene. The intense erosion of the metamorphic basement resulted in the formation of a plane surface, creating a part of the Aegean continental shelf during the Oligocene and Miocene.

The limited thickness of the Neogene sequence (Upper Miocene-Lower Pliocene), and the absence of clastic material, indicate an uplift of the area for extended periods (Fytikas, 1977; Markopoulos & Katerinopoulos, 1986).

During the Middle and Late Pliocene, the area of Milos was affected by an extensive volcanism, which was more or less continuously active. Phreatic explosions took place until recent and historic times (Angelier et al., 1977; Fytikas et al., 1984; Fytikas et al., 1986; Traineau & Dalabakis, 1989).

The volcanic succession of Milos overlies the Mesozoic metamorphic rocks and the Neogene limestones (Fig. 3). It comprises a thick (up to 700m) (Fytikas & Marinelli, 1976) compositionally and texturally diverse Upper Pliocene-Pleistocene succession of calc-alkaline volcanic rocks, that record a transition from a relatively shallow, but dominantly below-wave-base submarine setting, to a subaerial one. The felsic-intermediate volcanic succession comprises syn-volcanic intrusions, lava domes and volcanoclastic rocks, which host several significant epithermal gold deposits. The growth and development of submarine felsic volcanoes are difficult to observe, while records of phreatic eruptions are extremely restricted.

The most recent attempts to describe the volcanic succession on Milos were those of Fytikas & Marinelli, 1976; Angelier et al., 1977; Fytikas, 1977; Fytikas et al., 1984; Fytikas, 1979.

The following formations have been distinguished:

a) Volcano-sedimentary rocks, consisting of pyroclastic material, pumice flows, tuffs, and tuffites. It is a thick (>120m) succession of felsic, pumice-rich, submarine units (Angelier et al., 1977; Fytikas et al., 1986), which represent the earliest volcanic activity (Middle-Late Pliocene).

b) Domes and lava flows. The effusion of lavas, the composition of which is rhyolitic to andesitic, was accompanied by the ejection of pyroclastic material, and the emission of glowing avalanches (Late Pliocene-Early Pleistocene).

c) Lavas from the recent volcanic activity. Their composition is rhyolitic to rhyodacitic. They are the products of a mainly eruptive activity, which resulted in the deposition of successive layers of lava, pumice, and cinders.

d) "Green lahar". A strange, chaotic formation, consisting of angular fragments of metamorphic rocks and, more rarely, volcanic pebbles. The fine bonding material is usually of volcanic origin. In a few cases, though, it is the product of the alteration of the metamorphic rocks.

e) Rhyolitic products of a tuff ring in fall and surge deposits, together with important lava flows of the same composition, are the younger deposits (90 ka).

f) Tuffites, which indicate the end of the volcanic activity.

Volume n° 4 - from P14 to P36

Petrology and Chemistry of the volcanic rocks

As mentioned above, the volcanic formations on Milos belong to the calc-alkaline association. Most rocks are andesites, dacites, and rhyolites; basalts are completely absent and basaltic andesites are rare.

Nearly all the volcanic products are porphyritic; only some rhyolitic members are completely glassy. In the less evolved rocks, phenocrystals are typically represented by zoned plagioclase, generally augitic clinopyroxene, orthopyroxene, and magnetite microphenocrysts. Unstable olivin and hornblende are sporadically present. The ground mass always contains a variable amount of glass, together with the same phases forming the phenocrysts. In the dacitic rocks, the phenocrysts are characterized by plagioclase, orthopyroxene, and clinopyroxene; hornblende appears widely spread and there are occasionally rims of clinopyroxene; biotite and strongly corroded quartz are sporadically observed.

The variability in the chemistry of the more evolved rocks (rhyolites more recent than 1 Ma), seems particularly significant. Two main groups can be distinguished:

a. Low-Ca rhyolites, showing CaO contents usually lower than 1%, thus with normative anorthite of around 2-3%, and the Na_2O/K_2O ratio < 1; the petrographical observations suggest a plagioclase-quartz-sanidine sequence of crystallization of sialic minerals; femic minerals are essentially represented by biotite.

b. High-Ca rhyolites: these rocks show CaO contents invariably greater than 1%, with normative anorthite ranging from 5% to 11%; the Na_2O/K_2O ratio > 1; sialic phenocrysts are represented by plagioclase and quartz, sanidine being typically absent; femic minerals are biotite and amphibole, present only in older products.

The first of the two distinct groups (low-Ca rhyolites), is typical of the Trachilas complex, whereas the second is observed in the Halepa and Fyriplaka eruptive systems. Systematic sampling showed reasonable homogeneity within each individual eruptive system, as regards both the major and trace elements. This suggests the lack of any major zonation, within the magma chamber, which fed the volcanic activity.

Conclusions on Volcanology

The volcanic activity began in the western part of Milos island with submarine eruptions, which later evolved to subaerial ones, covering a time span from 3,5 to 2,0 m.y. before present. Subsequently, igneous activity moved to the northeastern part of the island, where submarine pyroclastic products were deposited jointly with the extrusion of subordinate subaerial or submarine domes (1,8-1,0 Ma). Then, the volcanic activity reduced, and became concentrated in the central part of Milos. It was affected by strong tensional tectonics. The latest volcanism is dated at 0,1 million years before present (Fyriplaka Volcano).

Products ranging from basic andesites to rhyolites, with a clear dominance of the intermediate members, characterize the Pliocene volcanic cycles. The major and trace element variations, together with the isotopic ratios available, suggest that this rock association originated from a complex process of contamination and fractional crystallization. The absence of large central volcanic structures, the different composition of practically coeval eruptions, the minor role played by the plagioclase in the fractionation process, have been interpreted as evidence for a feeding system, relatively deep in the crust, from which small masses of magma originated separately, each rising to the surface to form domes and pyroclastics in the western part of the island. The subsequent cycle of activity (Early Pleistocene) was fed by a new input of deep magma, starting with the emplacement of more evolved products. The composition of the volcanics then became exclusively rhyolitic during a later phase of activity (Late Pleistocene), and progressively decreased in volume.

According to the petrographical, geochemical, and isotopical data, the origin of the more evolved members is compatible with processes, mainly due to the fractional crystallization dominated by plagioclase, in which contamination was decidedly subordinated.

In conclusion, all the collected and analyzed data suggest different trends for the older (Pliocene) and younger (Pleistocene) phases of activity. The *first phase* is related to a main feeding system set in a deep part of the crust or at the crust-mantle boundary, basically outside the range of plagioclase stability. The volume of this deep chamber must have been relatively large, permitting its existence for a relatively long period (about 1,5 million years) as well as allowing for important processes of assimilation of the crust rocks. The *younger phase*, on the other hand, seems to be related to multiple feeding systems, each of modest volume, and being relatively shallow and of short life, and therefore avoiding consistent interaction processes with the crust rocks.

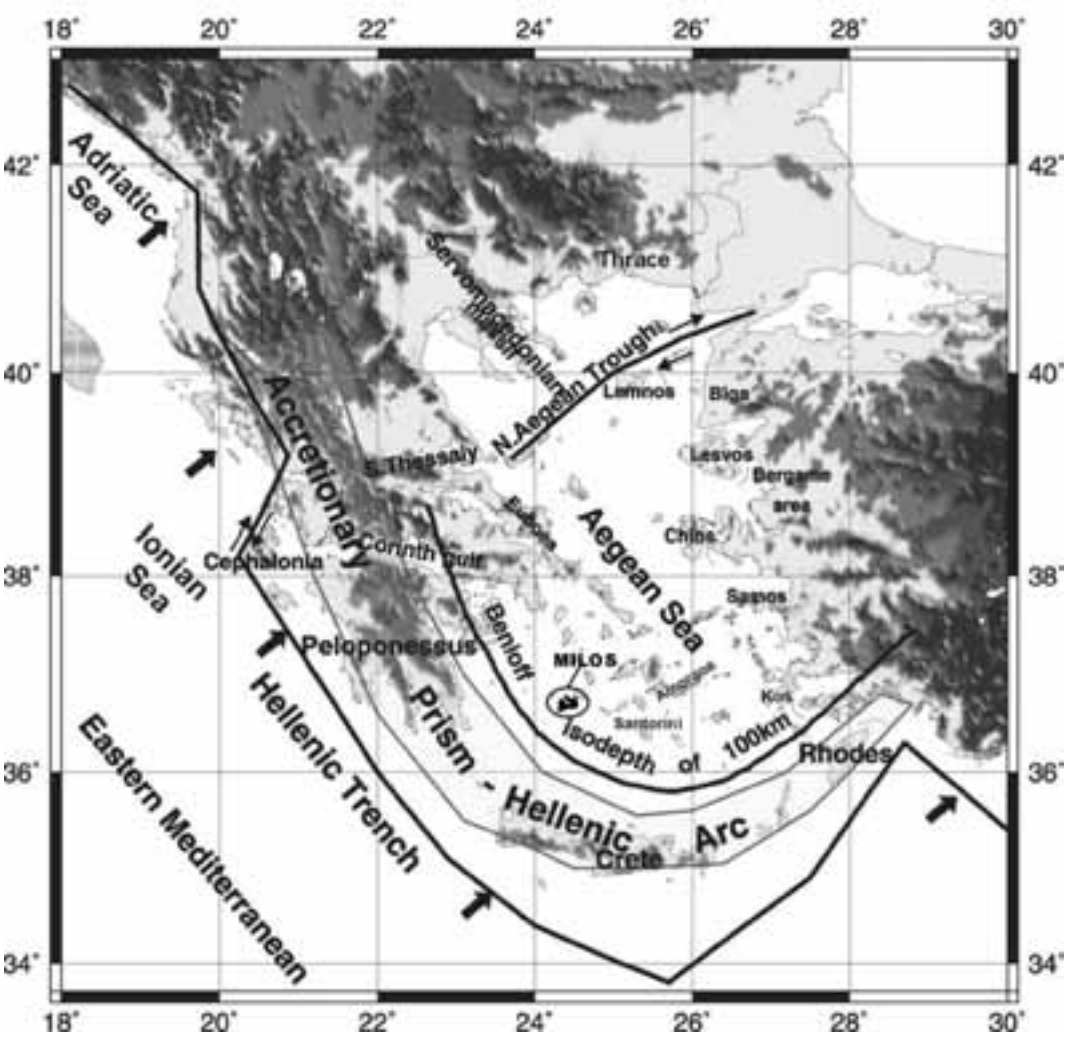

Figure 1 - Geodynamic situation of Greece and the location of Milos Island on the Aegean volcanic arc (Papazachos, Papazachou, 2001)

This different evolution of the feeding system in the two main phases of volcanic activity on Milos is interpreted as a consequence of consistent variations in the stress field affecting the crust. In fact, during Late Pliocene times, this sector of the Arc was affected by a relatively weak tensional tectonic regime, as observed in the Aegean area, where a compressional episode has been described at the Pliocene-Pleistocene boundary (Mercier, 1981).

Tectonic-Neotectonic activity

The tectonic structures in the area of Milos were mainly affected by the Alpine orogenesis. Due to the new geotectonic situation, the area was also influenced by further intense tectonic activity during the Pliocene and Quaternary. Milos presents an interesting seismic activity, which indicates the neotectonic and active character of the tectonic structures. The study of the tectonic situation of the island has substantially helped towards a better understanding of the volcanological situation, the stratigraphy, and the recent and active thermal conditions.

The ascension of magma is attributed to a strong tensional tectonic regime. The effects of such tectonics have been mapped by Fytikas on a scale of 1:25.000 (IGME, Geological Map of Milos Island, 1977). A

Volume n° 4 - from P14 to P36

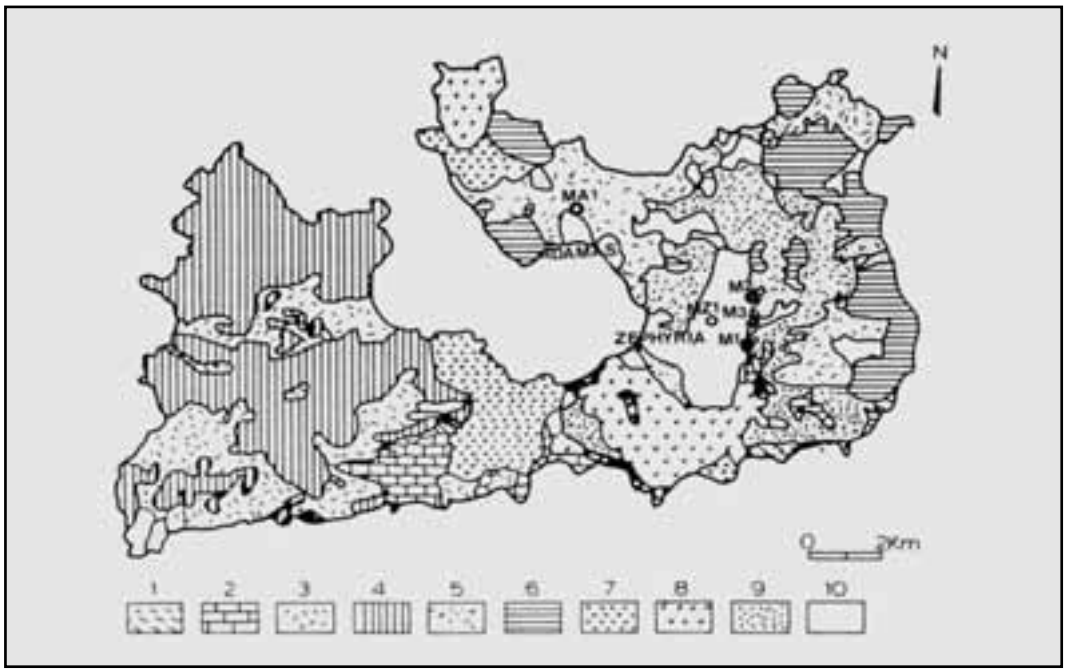

Figure 2 - Simplified geological map of the island: (1) Metamorphic basement (Middle-Upper Pleiocene), (2) Transgressive marine sediments (Upper Miocene - Lower Pliocene), (3) Basal pyroclastic series (Middle-Upper Pliocene), (4) Complex domes and lava flows, (5) Pyroclastic series (lower Pleistocene). (6), (7) Lava domes. (8) Rhyolitic complexes (Upper Pleistocene), (9) Products of phreatic activity, (10) Alluvium. The locations of the deep boreholes are marked (Fytikas, 1977; 1989).

dense grid of faults, grabens, and horsts can be easily observed both in the field and in aerial photographs. The frequent earthquakes and the sinking of the pre-historic and historic constructions under the sea show that the tectonism is still active today.

According to the detailed neotectonic study of Milos by Simeakis (1985), three phases of tectonic activity can be distinguished:

1. Pliocene: **distensional** tectonics with a general NE-SW direction.
2. Post-Pliocene: **compressional** phase
3. Quaternary: intense **extensional tectonics** with a general NW-SE direction

The last phase play a significant role in the neotectonic evolution of the area, and consequently to the facilitation of both volcanic activity and the circulation of thermal fluids. The most recent faults, which are more common in eastern Milos, follow the ENE-WSW direction, and are intersected by the older NW-SE faults, which correspond to the major Pliocene episodes, thus influencing greatly the volcanism, structures and geothermal situation of the island (Fig. 4).

The mild extensional regime favored the accumulation and stagnation of calc-alkaline melts at depth (probably at the bottom of the crust), which acted as a filter system in such a geodynamic context. From the Pleistocene, the tensional tectonics became more intensely active, allowing deep magmas to rise to shallow levels. The Pleistocene volcanic activity, characterized by small volumes of evolved magmas, above all homogeneous, and with a distinct petrogenetic history, is to be regarded as the result of a eruptive rate that, being comparable with the feeding rate of the deep magma, prevented the formation of large shallow magma chambers (Fytikas et al., 1986).

Hydrothermal activity

The results of the widespread hydrothermal activity (fossil and active thermal manifestations, craters of phreatic explosions, etc), are evident in the biggest part of Milos. The age of the hydrothermal activity is relatively recent, and is connected to Pleistocene phase tectonism and the great geothermal anomalies, the development of which is attributed to the formation of shallow magma chambers. The activity

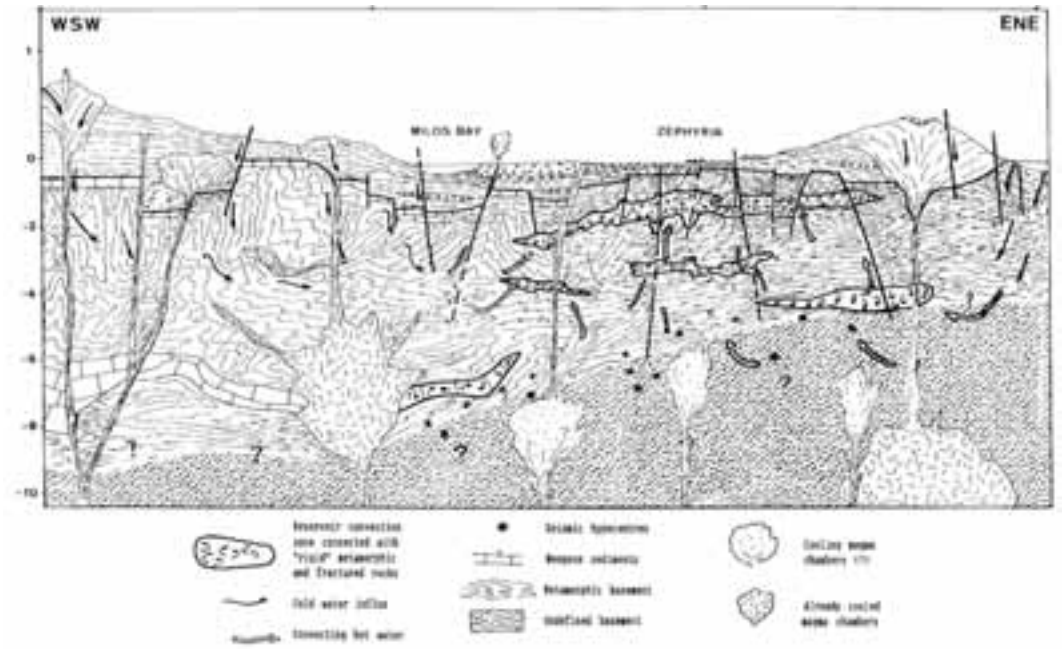

Figure 3 - Schematic geological profile across Milos island (Fytikas et al., 1989).

has let to the creation of several mineral deposits, both by transformation and deposition.

The most important effect of this, is the transformation of the volcanics into clay minerals. Depending on local conditions, we have "bentonization" in the deeper hot environment, and "kaolinization" in the shallower ones (Fytikas & Marinelli, 1976).

The temperature of the hydrothermal phases formation was initially around 100°C. As the permeability of the surface volcanites was reduced by "self-sealing", due to the thermal transformations, a progressive uplift of the isotherms took place. Thus, the presence of a good "cover", and hot hydrothermal fluids at shallow depths, resulted in the occurrence of phreatic explosions. By making simple considerations, the temperature necessary for such explosions for the craters north of Zephyria has been estimated to be 325°C. This estimation was later verified by the measurements in 5 production wells in the same area.

On the island several but small thermal manifestations can be observed: fumaroles, hot springs, hot grounds, submarine gas escapes. They are mainly located in the central and eastern part of Milos, and occasionally on the sea bottom. The maximum measured temperature of the fumaroles is 101°C, of the hot grounds, 100°C (30cm below surface), and of the hot springs, 76°C.

Geothermal situation

Extensive geothermal exploration has been carried out in Milos since 1971 until today. It was started by the Institute of Geological and Mineral Exploration (IGME), and the Public Power Corporation (PPC) during the years 1971-1976.

This exploration program included 60 shallow (40-80m) slim thermometric wells, all around Milos, from which the mean geothermal gradient was defined (Fytikas, 1977; Fytikas, 1989). The observed gradient is high everywhere, but particularly in some areas of the central and eastern parts of the island, and its mean values are greater than 8°C/10m, in other words 24 or more times higher than the world average.

From the iso-gradient map (Fig. 5) that was produced, two main geothermal areas were distinguished: the **Zephyria** plane and the **Adamas** area, while some minor anomalies were observed in the western part of Milos. Southwards of Zephyria, where there are outcrops of the crystalline basement and superficial thermal manifestations, a strong anomaly is expected.

In the framework of this program, two deep exploration-production wells were drilled: MZ-1 in the Zephyria area (max. depth 1101m), and MA-1 in the Adamas area (1163m). Both wells produced a mixture of steam and liquid, proving the existence of

Volume n° 4 - from P14 to P36

a geothermal reservoir with a temperature of 310°C at a depth of 932m in MZ-1, and 250°C at a depth of 1095m in MA-1 (Fytikas et al., 1976).

During the years 1980-1982, three new wells were drilled in the Zephyria plain: MILOS-1 (1180m), MILOS-2 (1381m), and MILOS-3 (1017m) (Cataldi et al., 1982; Vrouzi, 1985; ENEL and PPC, 1981a, b, 1982). The results of the enthalpy measurements during the production tests on MILOS-2 in 1984 gave values of more than 1700KJ/kgr, thus revealing a maximum temperature of 318°C at a depth of 1150-1200m.

In 1985, PPC started the operation of a pilot geothermal power plant (2MW) in Zephyria, which was terminated in 1986, due to several operational problems, but mainly because of the local opposition to the environmental noise (mainly an H_2S smell). Recently, a new geothermal project has been started in Milos, which will exploit the very shallow (80-150m) low enthalpy (80-100°C) geothermal fluids for the desalination of seawater.

Industrial Minerals and Rocks of Milos

The formation of deposits of industrial minerals and rocks in the island of Milos is closely associated with the volcanic and hydrothermal activity, which is still present today in the form of thermal springs, mainly solfataras. However, bentonites and kaolins, the two main types of industrial mineral deposits formed by the alteration of the original volcanic rocks, are not related as far as their mode of formation is concerned (Fig. 6).

Kaolin deposits

The main mineral phase present in the kaolin deposits is kaolinate and/or halloysite. Both minerals are hydrous Al-silicates, with 1:1 layer structure (i.e. consisting of a tetrahedral layer following an octahedral one). Halloysite contains an additional sheet of water between the 1:1 layer units, which can be easily lost by heating at temperatures as low as 60°C (conversion to the anhydrous 7A-halloysite). Both kaolinite and halloysite are present in the kaolins of Milos.

The presence of other mineral phases in the kaolin deposits affects the physical properties of the raw materials, and depends on the type of the parent rock and the geological processes prevailing during the formation of the deposits. They usually include Ti- and Fe-oxides, micas, feldspars, smectites, and various polymorphs of silica; and sulphates, which deteriorate the physical properties of the deposits, especially those concerning their applications as fillers. The coarse-grained phases affect the abrasion characteristics of the materials, while the smectites cause rheological problems in the applications in the paper industry.

Sulphates like alunite, which are very common in the Milos deposits, cause further problems in ceramic applications, because SO_3^{-2} is released. The latter can be easily converted to sulphuric acid on firing.

The kaolin deposits of Milos belong to the category of primary kaolin, and have been formed in situ by the hydrothermal alteration of volcanoclastic rocks under acid conditions (Ph= 4-5). The deposits form pockets or lenses, and are controlled by structural criteria (faults, tectonic contacts).

The main phase is kaolinite and/or halloysite, associated with quartz, christobalite ± alunite ± barite ± halite ± Fe-oxides. Kaolinite is fine-grained (flakes smaller than 1μ.).

The relatively poor quality of the kaolin deposits of Milos, mainly due to their opaline silica and alunite content, renders them unsuitable for coatings and fillers. Only small quantities are consumed by these industries. The major application of the Miloan kaolin is the manufacture of white cement, where the high silica sulphate contents do not cause big problems.

The grade of the poor deposits can be improved as far as alunite is concerned, but the separation of Opal-CT, the grain size of which is very similar to that of kaolinite, is very difficult.

Bentonite deposits

Bentonites contain smectite as the major mineral phase. Smectites are 2:1 layer silicates (an octahedral sheet "sandwiched" between two tetrahedral sheets), with structures similar to pyrophyllite (dioctahedral smectites) and talc (trioctahedral smectites). However, unlike talc and pyrophyllite, smectites are characterized by cation substitutions in both the tetrahedral and octahedral sheets. These substitutions lead to a charge deficit, which is counterbalanced by the so-called interlayer cations. The latter are exchangeable, imparting the cation exchange capacity. The exchangeable cations are hydrated, causing swelling of the smectite layers. Cation exchange capacity and swelling are very important properties of the bentonites, and many applications of these raw materials are based on them.

Like the kaolin deposits, bentonites contain a variety

of clay and non-clay minerals, the presence of which depends on the type of the parent rock and geological processes which prevailed during their formation. The most common accessory minerals are feldspars (both K-feldspar and plagioclase), zeolites, various forms of silica polymorphs (with the most common representative phase being opal-CT), kaolinite and/or halloysite, mixed layered clay minerals, (most commonly, illite/smectite and less commonly, chlorite/smectite), and various sulphates and sulphides.

The bentonites of Milos consist principally of smectite (smectite contents of up to 95%). They contain authigenic and pyrogenetic K-feldspars, pyrogenetic plagioclase, opal-CT, zeolites, sulphates (gypsum, alunite, jarosite, barite), sulphides (pyrite and/or marcasite), Fe-oxides and Ti-oxides (mainly brookite). Smectites have a very variable composition, which is determined to some extent by the composition of the parent rocks; Beidellite and montmorilonite are present. Cheto and Wyoming type montmorillonites are present in the Miloan bentonites but they do not co-exist. Also, beidellites do not co-exist with Wyoming montmorillonites. The Miloan bentonites are predominantly Ca, Mg-rich. Na-activation is applied to improve their performance in their various different industrial applications.

The bentonite deposits of eastern Milos are more or less stratiformed, i.e. they are controlled mainly by stratigraphic and tectonic criteria. The presence of authigenic K-feldspar in the dissolution of cavity-fillings, and/or pore linings in several deposits, indicates that sometimes the alteration of the parent volcanoclastic rocks took place at very low temperatures. Furthermore, the hypothesis for the hydrothermal genesis of the deposits (mainly pyroclastics, but also lavas in origin) is the most probable, at higher temperatures (150-180°C) and under alkaline pH conditions. On the contrary, it is possible that some of the Miloan bentonites were formed by the devitrification of volcanic glass in a marine environment at low temperatures. Several deposits contain opaline-silica beds, which are not associated with hydrothermal activity, but are by-products of the devitrification of volcanic glass. Small bodies of non vitrified or partly vitrified galls are also present.

Almost all bentonite deposits have been affected by

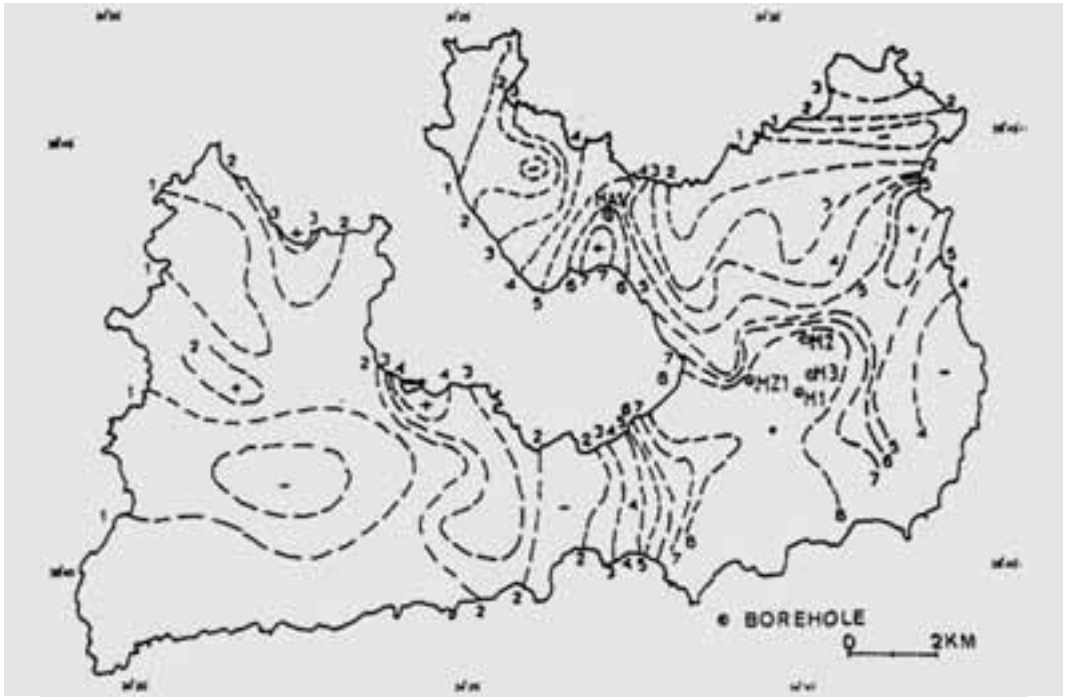

Figure 4 - Map showing the thermal gradient contours (dashed lines) along with the main visible faults (thin solid lines). The thick solid lines represent the faults obtained by the interpretation of the terraced gravity data (Tsokas,1996).

Volume n° 4 - from P14 to P36

hydrothermal activity. The influence of hydrothermal alteration is still visible today in the deposits of "Ankeria", in the form of sulfurous thermal springs and sulfa-tones.

Greece, due mainly to the Minoan bentonite, is a great producer of such hydrothermal products. The exact reserves are not known, but they are of the order of several tens of millions of tonnes. The major operating company in Milos is "Silver and Barite Ore Mining Co.", with a production of more than 850.000 tonnes per year. The raw material is dried in flat areas under atmospheric conditions, then activated by sodium carbonate, and finally by air-heating burners. The active period of bentonite extraction is between May and October.

The Miloan bentonites can be used successfully in the drilling industry, as a binding agent in the greensands, in iron-ore pelletization, in civil engineering applications, as animal litters, etc. White bentonites are present in eastern Milos in the area of Komia, but their quality is rather poor, because although their brightness is not low (75-85%), they contain abundant opal-CT. Detailed acid activation experiments have shown that they can successfully decolorize edible glyceride oils.

Barite deposits

Barite deposits are present principally in eastern Milos, in the form of veins filling faults. Their exploration began in 1934 and was associated with the beneficiation of silver as a by-product (baritine). Today, barite extraction has dropped to 30.000-50.000 tonnes/year. The actual reserves have been estimated at approximately 2,5 million tonnes of barites, with a specific gravity of 3,5 gr/cm^3.

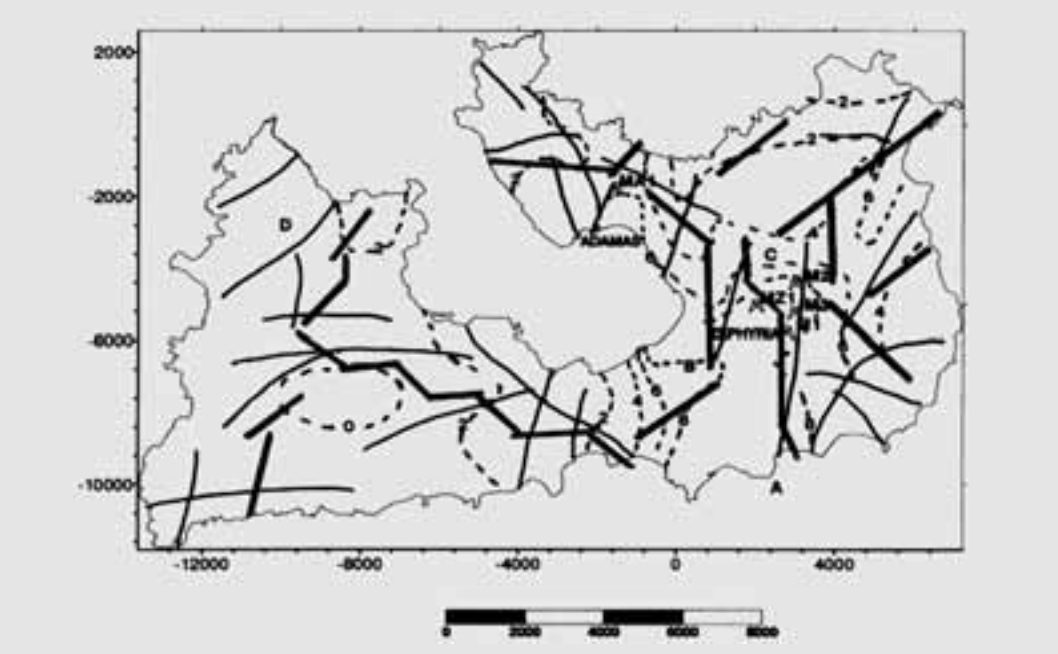

Figure 5 - Contours of the geothermal gradient on Milos island (oC/10m) (Fytikas, 1977).

The geological characteristics of barite deposits, and their special relationship with bentonites, indicate that their formation might postdate the formation of bentonites. In several locations (e.g. Agrilies and probably in the Tsantili deposit), the emplacement of barite is probably associated with K-metasomatism and subsequent illitization of the bentonite. In this way, the quality of the bentonites deteriorates and the formation of K-bentonite takes place (sub-bentonite). The illitisation reaction releases Si, which causes silicification to the surrounding rocks. Therefore, the silicified rocks observed in Milos are not necessarily associated entirely with the Si deposition, but are the product of the hydrothermal alteration-reaction.

Barite with manganese are also interesting deposits in Milos Island (Vani-marine deposits), in a beautiful volcano-sedimentary formation. On the

north-west part of Milos island, in the area of Cape Vani, a manganese and barite mineralization is present. The "occurrence" lies in a series of Upper Pliocene volcanoclastic materials with marine fossils (Argyropoulos 1966, Schmidt 1966, and Fytikas 1977), and it is divided into two phases.

The first phase contains ramsdellite and pyrolusite, while the second phase contains coronadite-cryptomelane-hollandite and hydrohetaerolite.

The main mineral phases are as previously cited. The accessory mineral phases are: arsenosiderite, barite, galena, pyrite, and sphalerite.

According to Liakopoulos (1987), the three main stages of Mn-minerals genesis can be distinguished:

During the first stage, Mn-solutions are discharged under submarine conditions, forming the MnO_2 minerals pyrolusite + ramsdelite. This stage is accompanied by the emplacement of very finely disseminated barite in the tuffs.

In the second stage, formation of the isostructural Mn-oxides (coronadite, cryptomelane-hollandite, and hydroheteroaerolite), took place. The oxides of the second stage are characterized by the presence of Ba, Pb, K, Zn, and As.

The third stage is defined by the formation of quartz + barite ± sulphide veins and carbonates + quartz ± sulphides. The geochemical analysis of the metalleogenic third phase, indicates that carbonates were placed in these veins at a temperature of 180°C, and that their formation required the mixing of the mineralized fluids with seawater.

Generally, the formation of the manganese and barite took place rapidly through the hydrothermal activity in the area of Cape Vani, probably after the submarine formation of the volcano-sedimentary sequence. The hot fluids penetrated to the previous formations by vertical fractures, and migrated along the bedding plane of the sediments, where they emerged (Liakopoulos et al, 2001).

Perlite deposits

The volcanic centers of Milos Island have created very

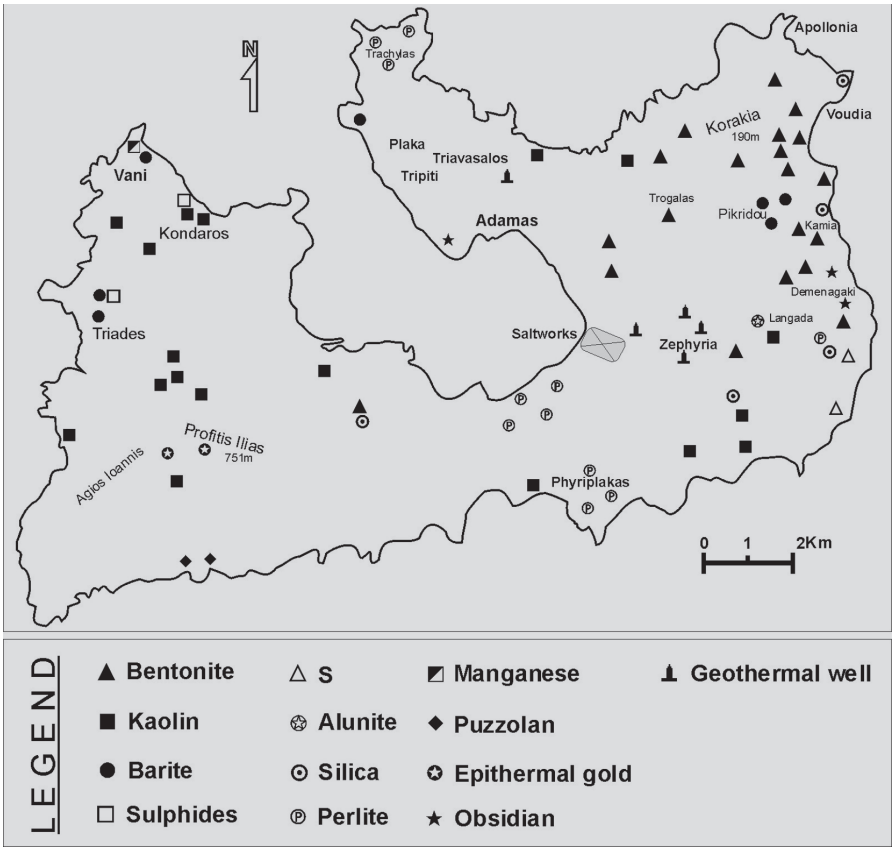

Figure 6 - Sketch map with the locations of the industrial minerals of Milos

Volume n° 4 - from P14 to P36

massive deposits of rhyolitic perlites (Argyropoulos & Fytikas, 1991). The perlites, were not influenced by the hydrothermal alterations, and formed the Chalepa lava dome and flows (1,2 Ma), the Trachylas tuff ring cone and lava flows (0,34 Ma), and the Fyriplaka tuff ring cone and lava flows (0,09 Ma). Smaller and less interesting outcrops of rhyolites, and in places, of perlitic lavas, are encountered at the Hondro Vouno, Bonbarda, and Demenegaki volcanic domes and flows.

The chemical composition of the most important rhyolites of Milos is given in Table 1 (Fytikas et al, 1986).

Trahilas center has produced low Ca rhyolites and plagioclase, and biotite phenocrystals, while the rhyolites of Tsigrando-Fyriplaka and Chalepa are rich in Ca, and rarely contain phenocrystals of plagioclases or biotite-amphibole. The basic mass is generally glassy.

The chemical composition of both the main and secondary minerals is stable, as it is in all the products of each volcanic center.

The perlite formations are settled with all three basic processes of volcanic activity: the eruptive, the extrusive and the effusive. In any of these cases, the eruptive-effusive perlites prevail over the other types, and form lava domes and thick lava flows. This is natural, since the activity was fed by intensively viscous acid magmatic material, from which, after the initial eruptive activity, the main bulk of its volatile substances was removed. Such domes and perlitic lava flows predominate in Milos (Chalepas, Trachilas, Vounalia, etc).

Perlitic volcanic products, created also by eruptive activity, formed cones of perlitic lapillis, as in the case of the Fyriplaka and Trahilas cones.

The hydration mechanism of the acid magma under submagmatic temperatures, has not been fully understood so far. The simplest hypothesis is that the magmatic mass absorbed the suspended (sea-, lake- or river) water, and that the water was either deposited or entered in the mass during its consolidation.

The perlite of Milos consists of quartz, feldspars, biotite, opaque minerals, vesicles, and glass (Koukouzas and Dunham, 1994). Various textures have been identified, ranging from the hard perlite texture, to the pumiceous one. The proportion of vesicles increases and glass decreases from the hard to the pumiceous perlite, indicating the hydration of glass. The supplies of all perlite types in Milos are very high.

The Trachilas perlite reserves are estimated to hold 184 Megatons, and the Fyriplaka reserves, 884 Megatons. The Chalepas perlites are considered to be less important, due to their quality, and also all the other perlites, due to their small quantity.

In the recent years, the perlite production in Milos is held only by the Silver and Barite Company, and is calculated at about 500,000 tonnes/year. For that, Milos is the second world's largest producer of perlite.

Puzzolan deposits

In the southwestern part of Milos Island, very important puzzolane deposits were discovered, laying on the pyroclastic formations outcropping there.

Two big Greek cement companies produce hundreds of thousands of tonnes of this interesting industrial volcanic product.

Epithermal gold deposits

The large-scale geothermal systems in Milos were structurally controlled, and precipitated spatially and temporally telescoped quartz-adularia-Fe, sulfide-gold systems by crack-seal mechanisms. The collapse of epithermal systems led to the dissolution of precious metals, and to the re-deposition of bonanza zones. Rare epithermal systems are massive siliceous replacements of 5 Ma evaporates and carbonate rocks. Some of the epithermal veins indicate the site of hydrothermal eruptions, while others formed steaming grounds, siliceous sinters, and boiling mud pools. Minor barite-argentian galena veins and hydrothermal eruption pipes occurred, associated with epithermal mineralisation (Plimer & Nethery, 2001).

Field itinerary

DAY 3

Arrival at Milos (noon or afternoon).

Introductory visits to the Geological-Mining Museum of Adamas, and to the industrial plants of Voudia (near Apollonia) are organized for the 1st day in Milos. In the Museum, the group will have the opportunity of watching a presentation on the geological and mining situation in Milos, using the appropriate facilities existing there, as well as seeing an important exhibition of mineral mining tools.

If there is enough time, there will be a visit to the northwestern part of the island, where the pyroclastic

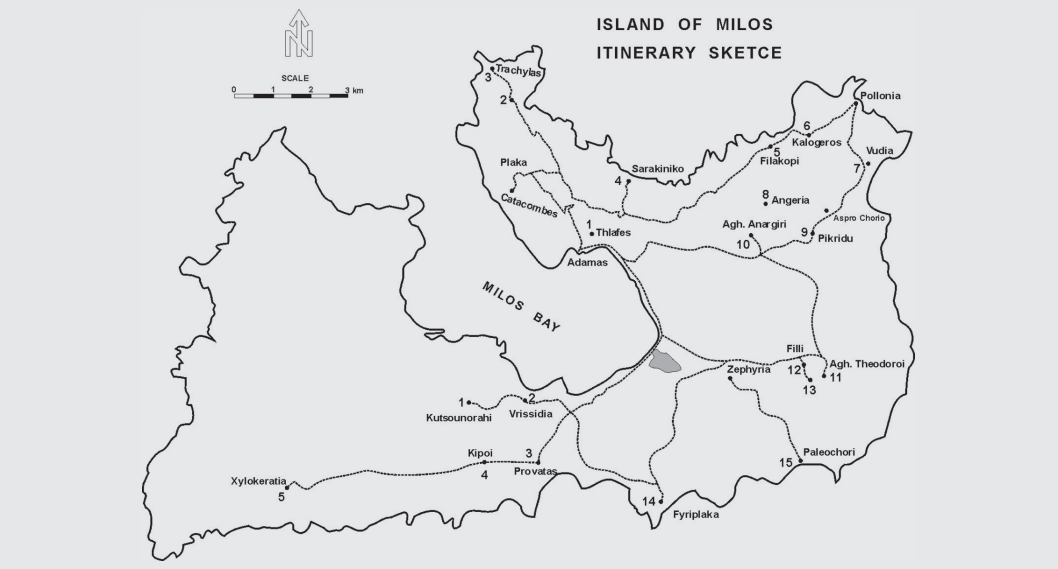

Figure 7 - Itinerary Sketch Map

formations of Sarakiniko and Bombarda, and the dacitic-andesitic lava domes and flows can be observed.

The ancient village, the Roman theatre and the paleo-Christian (2nd century AD) catacombs are built on the pyroclastic formations of the area.

In Plaka, the group could visit the mediaeval castle and some very old and interesting churches, which are constructed on the volcanic domes.

DAY 4

Departure from Adamas

Stop 1:

Thiafes.

600m northwards of Adamas downtown, there is a solfatara and hot ground field, with gas and soil temperatures at 100°C. The hot area is a result of the intersection of two important faults (N-S and E-W directions). Its size is 15000m^2 .

At a borehole drilled there, the temperature at the bottom (72m), was 138°C, and a water-steam mixture was produced. Deposits of S are visible in many spots.

Stop 2:

Trachilas tuff ring.

The external deposits of the Trachilas tuff ring are visible in detail. Numerous explosions caused the fragmentation of the original rhyolitic magma, and deposited it at the flames of the cone in a reverse-grating sequence. A lot of older lavic lithics can be observed.

Stop 3:

Trachilas perlite quarry (mine).

In the internal part of the cone, the rhyolitic lavas, that flow in a northwest directionto the seashore line, are to be found.

The lava has a typical perlitic structure, and it is one of the best quality perlites existing in the world. The exploitation is open-style; they use explosives and create continuous terraces. Some interesting rehabilitation work exists.

Stop 4:

Sarakiniko.

Natural erosion has created an impressive landscape, with pumice falls and fine-grained acid (white) pyroclastics. Marine fossils (Echinoderms, Lamellibranches, Brachiopods, etc), typical of a shallow marine environment, are abundant in the area. The collapse of the fine-grained tuffites, and the presence of faults and fractures on the white formations, helped the deposition of hydrothermal products inside these tectonic cracks. Kaoline formations are also present, as well as some gigantic pumice-stones (sometimes with a diameter bigger than 5m).

Volume n° 4 - from P14 to P36

Stop 5:

Phylakopi.

Near the prehistoric settlement of Phylakopi, typical outcrops of the pumice flow formation exist. Big pumices have formed a deposit up to 50m thick, together with a fine-grained volcanic ash matrix, mixed with very small pieces of pumice. The pumices are some imes higher than 2 m, and have a constant chemical composition. This formation is of marine origin.

Above this rhyolitic formation, there are gray-colored hyaloclastites with pseudo-pillows, which were formed in a shallow marine environment. Some white lithics come from the pumice formation. The hyaloclastites are linked to the adjacent volcanism, which formed submarine dacitic-crypto-domes.

Stop 6:

Kalogeros.

The external part of the dacitic crypto-dome (pentagonal columnar lavas, breccia, and mud-flow), can be clearly observed near the Adamas-Apollonia road.

Stop 7:

Vudia area.

The road passes near the facilities and installations of the Silver and Barite Company. The visitors will be able to see the air-drying of bentonite and the preparation of the mineral.

Stop 8:

Angeria and other quarries.

Passing through other bentonite mines (Aspro Chorio, and Tsantili), we will arrive at the Angeria quarry, which, together with the other two neighboring ones, could be the largest opencast (strip mining) bentonite mine (>2km long and 200m deep) in the world. Here, it is easy to see the entire geological cross-section, and to observe the details of the hydrothermal activity that caused bentonitization, kaolinitization, and silisification.

Stop 9:

Picridou.

In this stop, we will see the Baritine mine, from which the other ore has been excavated, using small tunnels and wells. One can make out from the surface the metal-bearing rocks, consisting of microcrystalline barite, saturating the altered volcanites in a mushroom-like form.

Stop 10:

Aghii Anargyri.

A large and well-preserved phreatic explosion crater, with a diameter of about 600m, is located in this area. Pieces of the basement, with interspersed fragments of limestone (more than 1 meter in diameter), came up to the surface after the explosion which initially caused the crater. It was estimated that the temperature of the hydrothermal activity, which caused the explosion and resulted in the formation of the crater, must have been about 325°C.

Stop 11:

Aghii Theodori.

Several small phreatic craters, which are in contact with each other, and sometimes one is within or overlapping the other, are situated in this area. The external diameter of their rim is generally small (up to 20m), while their ribs consist of bedded angular pieces of weathered white vulcanite. The point of the explosion must have been very superficial.

Stop 12:

Filli (green lahar).

In Filli, we will examine a significantly extended mudflow with considerable stratigraphic importance, 90% of which comprises angular metamorphosed green rocks, and pieces of limestone or vulcanite, all well-mixed within the same matrix. The formation is chaotic, ungraded, of stable thickness, but its composition is not of a typical lahar. We have, however, used this term as being the most verisimilar, since every other possibility has been excluded.

Stop 13:

Filli (kaolin quarry).

An important kaolin open mine is operating in the area, producing good quality kaolin. The original volcanic formation from which the kaolin deposits were formed belongs to the old fine pyroclastic formation. Very recent "green lahar" deposits overlay the kaolins.

Stop 14:

Fyriplaka dome.

In the profile of a perlite mine which is located in the external side of the new crater, we can observe the crater's structure–which is made up of pyroclastic layers, continually varying in size (periodical alteration of explosion intensity), – and its almost

total lack of matrix, together with the stability in its composition (rhyolitic, perlitic), etc. Taking into account its enormous diameter (1700m), the fragility of its products, and their glass-like structure, it can be said that Fyriplaka is probably a submarine volcano of acid hyaloclastits. However, all the above-mentioned could be attributed to the abrupt contact between the seawater and the magma inside the faulted basement, and, thus, the crater could have been formed on dry land but near the sea. Its age is approximately 0.5 m.a.. Inside the Fyriplaka crater, another smaller and similar crater exists, as well as various lava flows of the same composition and a peculiar lahar, which mainly consists of pyroclastic materials from the biggest crater. The lava flows have moved in various different directions (however, mainly towards the NW), governed by whatever obstruction they confronted that eventually forced them to form small hills (which the natives call Vounalia).

Stop 15:

Paleochori.

In the Paleochori area, we can observe the metamorphic basement, some kaolin quarries, and the upper part of the Pyriplaka deposits. There is also a beautiful beach for an optional brief swimming stop.
On that particular beach, there is a certain spot where the sand temperature is approximately 100^{o}C, conditions that favor a great deal a kind of "geothermal cooking".

DAY 5

Stop 1:

Coutsounorachi.

The Mesozoic limestone basement, that follows an E-W direction, emerges from the volcanic formations, above them the Neogene limestones. The outcrops of the schists are limited.

Stop 2:

Vrissidia.

In Vrissidia, the older rhyodacitic lavas of the great extrusive complex of domes and lava flows of Halepa, are found. There is more than one lava flow, and these flows follow various directions. In this particular location, they have moved towards the NE, while at the back of the big main dome, they moved towards the south. The age of this complex has been determined, by K/At method, to 1.13+0.10 m.y., by using the relatively great amount of biotite phenocrystals. The sheeting of the lavas is characteristic of this type of volcano.

Stop 3:

Provatas

The Neogene sediment sequence starts with a multicolored basal conglomerate, and continues with marine deposits of marls, limestone, sandstones, etc. The area is characterized by impressive extensional faults, dipping to the north, which have created the unique morphology of the area. Many marine fossils can be found here.

Stop 4:

Kipoi

The volcanic dome of Chalepa has produced very well preserved thick lava flows of rhyolitic-rhyodacitic composition. The lava flow extends to the south and arrives at the actual shoreline. The lava structure and its well-developed phenocrystals are clearly visible.

Stop 5:

Xylokeratia

Following the road near the southern coast and going west, we pass through the Neogene deposits and volcanic formations of various origins: andesite lava flows, breccias from collapsed domes, mudflows, pyroclastics, etc.
Near Xylokeratia, we arrive at two very large quarries of puzzolan, a fresh pyroclastic formation, mainly composed of pumice breccias, volcanic ash, and (rarely) lithics from older volcanites.
There are two cement companies operating here, having an intensive activity and appropriate facilities to put the product directly into cargo containers, and carry it away by boat.
The group could visit both or one of these quarries (depending mainly on the time left).
The field trip ends at about midday, the participants will go back to Adamas, to prepare their departure from Milos by high-speed boat or airplane.

Acknowledgments

The elaboration of this guide was supported by the Ministry of Environment and Water of the Republic of Bulgaria and by the French-Bulgarian project RILA-4, involving the cooperation between EGIDE (France), and the Ministry of Education and Sciences of Republic of Bulgaria.

References cited

Aleksiev, B. (1968). Clinoptilolite des Rhodopes du nordest. *Comptes rendus de l'Académie bulgare des Sciences* 21, 1093-1095.

Angelier, J., Cantagrel, J.M., D. Vilminot, J.C. (1977). Neotectonique cassante et volcanisme plioquaternaire dans l'arc égeén interne: I'lle de Milos (Gréce). *Bull. Soc. Geol. France*, 19, 119-121.

Argyropoulos, G. and Fytikas, M., (1991). Perlites of Milos Island (Greece). *In: Proceedings of Perlite Meeting,* 4-6 May 1991, Hotel Hilton, Athens.

Bagdassarov, N.S. and Dingwill, D. B. (1994). Thermal properties of vesicular rhyolite. *Journal of Volcanology and Geothermal Res*earch 60, 179-191.

Bagdassarov, N., Ritter, F. and Yanev, Y. (1999). Kinetics of perlite glasses degassing: TG and DSC analysis. *Glass Sciences and Technol*ogy 72, 277-290.

Bontscheff, St. (1897). Das Tertiärbecken von Haskovo (Bulgarien). *Jahrb. Geol. Reichsanstalt*, Bd. 46, H2, 309-385.

Calas, G., Angelov, S., Yanev, Y. and Kostov, R.I. (1988). Electron paramagnetic resonance of perlites from Eastern Rhodopes, Bulgaria. *Geologica Balcanica* 18 (5), 53-60.

Christidis, G. and Markopoulos, Th. (1992). Kaolinite generating processes in the Milos Bentonites and their influence on the physical properties of bentonit. *6th Congress of the Geol. Soc. of Greece*, p.13.

Dabovski, H., Harkovska, A., Kamenov, B., Mavroudchiev, B., Stanisheva-Vassileva, G. and Yanev, Y. (1991). Geodynamic model of the alpine magmatism in Bulgaria. *Geologica Balcanica* 21 (4), 3-15.

Dimitrov, V., Yanev, Y. and Dimitrova-Pankova, M. (1984). IR-spectroscopy of Eastern Rhodopes perlites. *Geochemistry, Mineralogy and Petrol*ogy, Sofia 19, 86-96 (in Russian with an English abstract).

Djourova, E.G. and Aleksiev, B. (1990). Zeolitic rocks related to the second acidic Paleogene volcanism to the east of the town of Kurdjali. In: "*Geologica Rhodopica, 2nd Hellenic-Bulgarian Symposium",* (S. Konstantinos Ed.). 2, pp. 279-489. Aristotl Univiversity, Thessaloniki, Greece.

Dormann, J.-L., Djega-Mariadassou, C., Yanev, Y. and Renaudin, P. (1989). Mössbauer study of mineral glasses: East Rhodopes perlites. *Hyperfine Interaction*s, J. C. Baltzer A. G., Basel 6, 651-658.

DruittT. H. and Sparks, R.T.J. (1982). A proximal ignimbrite breccia facies on Santorini, Greece. *Journal of Volcanology and Geothermal Research* 13, 147-171

ENEL and PPC (1981a). Milos Geothermal Project, *Report on well MILOS-1. GR/MI-9*, May 1981.

ENEL and PPC (1981b). Milos Geothermal Project. *Report on well MILOS-2. GR/MI-11*, July 1981.

ENEL and PPC (1982). Milos Geothermal Project. *Report on well MILOS-3. GR/MI-14*, January 1982.

Fytikas, M., Kouris, D., Marinelli, G. and Surgin, J. (1976). Preliminary geological data from the first two productive geothermal wells drilled at the island of Milos. *Proceedings of the International Congress of Thermal Waters, Athens, October 1976*, pp. 511-515.

Fierstein, J. and Hildreth, W. (1992). The Plinian eruption of 1912 at Novarupta, Katmai National Park, Alaska. *Bulletin of Volcanology* 54, 646-684.

Fuhrman, M. and Lindsley, P. (1988). Ternary feldspar modeling and thermometry. *American Mineralogist* 73, 201-215.

Fytikas, M. (1977). Geological and geothermal study of Milos Island. *IGMR*, Vol. XVII, No 1.

Fytikas, M. and Marinelli, G. (1976). Geology and geothermics of the island of Milos (Greece). IGME, *Proc. Geotherm. Energy* 1: 516-524.

Fytikas, M., Innocenti, F., Manetti P., Mazzuoli, R., Peccerilo, A. and Villari, L. (1984). Tertiary to Quaternary evolution of volcanism in the Aegean region. *The Geological Evolution of the Eastern Mediterranean (Edited by Dixon, J.E. and Robertson, A.H.F.), Geological Society of London, Special publication* No. 17, pp. 687-699, Blackwell, Oxford.

Fytikas, M., Innocenti, F., Kolios, N., Manetti P., Mazzuoli, R., Poli, G., Rita, F. and Villari, L. (1986). Volcanology and petrology of volcanic products from the island of Milos and neighboring islets. *J. Volcanol. Geotherm. Res.* 28, pp. 297-317.

Fytikas, M. (1989). Updating of the geological and geothermal research on Milos island, *Geothermics* 18, pp. 485-496.

IGME (1977). Geological Map of Milos Island, 1: 25.000.

Georgiev, V., Milovanov, P. and Monchev, P. (2003). K-Ar dating of the magmatic activity in the Momchilgrad volcanotectonic depression. *Comptes rendus de l'Académie bulgare des Sciences* 56 (8), 49-54.

Gogishvili, V.G. (1980). Epigenetic character of stratified deposits of highly-siliceous zeolites (on example of the Transcaucasus). In: "*Prirodnie Tzeoliti" (Natural Zeolites)* (Kossovskaya, A.G., Ed), pp. 65-75. Nauka Ed. House, Moscow (in Russian).

Goranov, A., Vutkov, V. and Petrov, P. (1960).

The perlites in the Eastern Rhodopes. *Izvestia na Geologicheskia Institut, Bulgarian Academy of Sciences* 7, 323-345 (in Bulgarian with an English abstract).

Hanski, E. J. (1993). Globular ferropicritic rocks at Pechenga, Kola Peninsula (Russia): Liquid immiscibility versus alteration. *Lithos* 29, 197-216.

Harkovska, A., Yanev, Y. and Marchev, P. (1989). General features of the Paleogene orogenic magmatism in Bulgaria. *Geologica Balcanica* 19 (1), 37-72.

Hervig, R.L., Dunbar, N., Westrich, H.R. and Kyle, P.R. (1989). Preeruptive water contents of rhyolitic magmas by ion microprobe analysis of melt inclusions in phenocrysts. *Journal of Volcanology and Geothermal Res*earch 36, 293-302.

Innocenti, F., Manetti, P., Peccerilo, A. and Poli, G. (1981). South Aegean Volcanic Arc: Geochemical variations and geotectonic implications. *Bull. Volcan.* Vol. 44 No 3, pp. 371-391.

Innocenti, F., Manetti, P., Peccerilo, A. and Poli, G. (1979). Inner Arc volcanism in NW Aegean Arc: geochemical and geochronological data. *Neues Jahrbuch Fur Mineralogie Mnashefte H4*. pp. 145-158

Ivanov, R. (1960). Magmatism of the Eastern Rhodope depression. Part I-Geology. *Trudove varhu Geologiata na Bulgaria, Seria Geohimia y Polezni Izkopaemi* 1, 311-387 (in Bulgarian with a German abstract).

Kocik, J., Nebrensky, J. and Fanderlik, I. (1983). *Colour of the glasses*. Stroyisdat, Moskow, 212 p. (in Russian).

Koukouzas, N. and Dunham, A., (1994). Genesis of a Volcanic Industrial Rock, Trachilas Perlite Deposit, Milos Island, Greece. *Bull. of the Geological Society of Greece,* Vol. XXX/3, pp. 333-340.

Lilov, P., Yanev, Y. and Marchev, P. (1987). K-Ar dating of the Eastern Rhodopes Paleogene magmatism. *Geologica Balcanica* 17 (4), 49-58.

Makropoulos, Th. and Katerinopoulos, A. (1986). Die Alunit-Vorkommen von Milos (Griecheland): Mineralbestand und Genese. *Chem. Erde* 45, pp. 105-112.

Makropoulos, Th. and Katerinopoulos, A. (1988). Mineralogical and petrographic study of samples from wells in the geothermal field of Milos island. *Submitted report to the Public Power Corporation Greece.*

Marakushev, A.A. and Yakovleva, E.B. (1980). On the origin of perlites. *Vestnik Moskovskogo Universiteta, Seria Geologicheskaia* 1, 3-18 (in Russian).

McKenzie, D.P. (1978). Active teconics of the Alpine-Himalayan belt: the Aegean Sea and surrounding regions. *Geophys. J. R.* Astron Soc. pp. 217-254

McPhie, J. and Stewart A. (2003). Shallow submarine felsic volcanism, Milos, Greece. Presented in the Intern. Conf. on The South Aegean Active Volcanic Arc: Present knowledge and future perspectives (SAAVA 2003), Milos island 17-20 Sept. 2003.

Mercier, J.L. (1981). Extensional-compressional tectonics associated with the Aegean Arc: comparison with the Andean Cordillera of South Peru-North Bolivia. *Philos. Trans. R. Soc. London. Ser*. A. 300, pp. 337-355.

Mercier, J. L., Sorel, D., Vergely, P., Simeakis, K. (1989). Extensional tectonic regimes in the Aegean basins during Cenozoic. *Basin Res.* 2. pp. 49-71

Moore, D.M. and Reynolds, R.C. (1997). *X-ray Diffraction and the Identification and Analysis of Clay Minerals*. Oxford Univ. Press, 378 p.

Papazachos, B.C., Papazachou, C.B. (1997). The Earthquakes of Greece. *Ziti Publ.*, Thessaloniki, Greece, pp. 304.

Noble, D.C. (1967). Sodium, potassium and ferrous iron contents in some secondarily hydrated natural silicic glasses. *American Mineralogist* 52, 280-286.

Peccerillo, A. and Taylor, R.S. (1976). Geochemistry of Eocene calc-alkaline volcanic rocks from the Kastamonu area, N. Turkey. *Contr. Miner. Petrol.* 58. pp. 63-81.

Pe Piper, G., Piper, D.J.W., Reynolds, P.H. (1983). Regional implications of geochemistry and style of emplacement of Miocene I-type diorite and granite, Delos, Cyclades, Greece. *Lithos* 60. pp. 47-66.

Plimer, I. And Nethery J., (2001). Epithermal Gold Deposits, Milos, Greece. *In: Proceedings of 4th International Symposioum on Eastern Mediterranean Geology,* 21-25 May 2001, Isparta, Turkey.

Simeakis, C. (1985). Neotectonic evolution of the Milos island complex. *IGME Report (in Greek)*, p. 50.

Popov, S., Janeva, J., Russev, K. and Bocev, P. (1989). Evaluation des perlites du Rhodope oriental comme matière première dans la production d'agrégats pour les bétons légers. *Ore-forming Processes and Mineral Deposits*, Sofia 30, 46-64 (in Bulgarian with a French abstract).

Raynov, N., Popov, N., Yanev, Y., Petrova, P., Popova, T., Hristova, V., Atanasova, R. and Zankarska, R. (1997). Geological, mineralogical and technological characteristics of zeolitized (clinoptilolitized) tuffs

deposits in the Eastern Rhodopes, Bulgaria. In "*Natural Zeolites, Sofia'95*" (G. Kirov, L. Filizova and O. Petrov Eds.), pp. 263-275. Pensoft, Sofia-Moscow.

Roedder, E. (1979). Silicate liquid immiscibility in magmas. In "*The Evolution of the Igneous Rocks. 50th Anniversary Perspectives"* (H.S. Yoder, Ed.), pp. 15-57. Princeton Univ. Press, Princeton.

Scholze, H. (1959). Der Einbau des Wassers in Glassern II. *Glastechn. Ber*. 32, 142-152.

Sheppard, R.A. and Hay, R.L. (2001). Formation of zeolites in open hydrologic systems. *In: "Natural Zeolites: Occurrence, Properties, Applications". Reviews of Mineralogy and Geochemistry* **45** (Bish, D.L. and Ming, D.W. Eds), pp. 261-275. Miner. Soc. of America, Geochem. Soc.

Steward, D. B. (1979). The formation of siliceous potassic glassy rocks. In "*The Evolution of the Igneous Rocks. 50th Anniversary Perspectives*" (H.S. Yoder, Ed.), pp. 339-350. Princeton Univ. Press, Princeton.

Taylor, M. and Brown, G.E.Jr. (1979). Structure of mineral glasses – I. The feldspar glasses $NaAlSi_3O_8$, $KAlSi_3O_8$, $CaAl_2Si_2O_8$. *Geochimica and Cosmochimica Acta* 43, 61-75.

Traineau, H. and Dalabakis, P. (1989). Mise en evidence d' une eruption phreatique historique sur l' ile de Milos (Greece). *C-R Acad. Sci. Paris*. pp. 1-308

Utada, M. (2001) Zeolites in burial diagenesis and low-grade metamorphic rocks. In: *"Natural Zeolites: Occurrence, Properties, Applications". Reviews of Mineralogy and Geochemistry* **45** (Bish, D.L. and Ming, D.W., Eds), pp. 277-304. Mineral. Soc. of America, Geochem. Soc.

Vrouzi, F. (1985). Research and development of geothermal resources in Greece: Present statues and future prospects. *Geothermics* 14, pp. 213-227.

Yanev, Y. (1970). Sphéruloids de rhyolites du volcan de Studen Kladénetz de l'Oligocène dans le Rhodope de l'Est. *Bulletin of the Geological Institute, Series Geochemistry, Mineralogy and Petrography* 19, 201-219 (in Bulgarian with a French abstract).

Yanev, Y. (1987). Characterization of volcanic glasses from the Eastern Rhodopes, Bulgaria. In "*II*nd *International Conference on Natural Glasses"*, pp. 129-138. Univ. Karlova Ed., Prague.

Yanev, Y. (1994). Cesium-bearing perlites from the Borovitza caldera in the Eastern Rhodopes, Bulgaria. *Petrology* 2 (1), 82-97.

Yanev, Y. (1998). Petrology of the Eastern Rhodopes Paleogene acid volcanics, Bulgaria. *Acta Vulcanologica* 10 (2), 265-278.

Yanev, Y. (2000). Immiscibility in the acid lavas. In: "*31st IGC. Abstract*", Section 6-7.

Yanev, Y. and Bardintzeff, J.-M. (1996). Dynamismes éruptifs du volcanisme paléogène de collision des Rhodopes orientaux (Bulgarie). *Comptes-Rendus de l'Académie des Sciences de Paris* 322, IIa, 437-444.

Yanev, Y. and Pecskay, Z. (1997). Preliminary data on the petrology and K-Ar dating of the Oligocene volcano Briastovo (Eastern Rhodopes). *Geochemistry, Mineralogy and Petrol*ogy, Sofia 32, 59-66.

Yanev, Y. and Zotov, N (1996). Infrared spectra of water in volcanic glasses. *Experiment in GeoSciences*, Moscow 5 (2), 1-9.

Yanev, Y., Karadjova, B. and Andreev, A. (1983). Distribution of alkalis and genesis of the acid volcanic rocks in part of East Rhodopes Paleogene depression. *Geolgica Balcan*ica 13 (3), 15-44 (in Russian with an English abstract).

Yanev, Y., Innocenti, F., Manetti, P. and Serri, G. (1998a). Upper Eocene-Oligocene collision-related volcanism in Eastern Rhodopes (Bulgaria)-Western Thrace (Greece): Petrogenetic affinity and geodynamic significance. *Acta Volcanologica* 10 (2), 279-291

Yanev, Y., Stoykov, S. and Pecskay, Z. (1998b). Petrology and K-Ar dating of the Paleogene magmatism in the region of the villages Yabalkovo and Stalevo, Eastern Rhodopes volcanic area. *Geochemistry, Mineralogy and Petrol*ogy, Sofia 34, 97-110 (in Bulgarian with an English abstract).

Zotov, N., Dimitrov, V. and Yanev, Y. (1989). X-ray radial distribution function analysis of acid volcanic glasses from the Eastern Rhodopes, Bulgaria. *Physics and Chemistry of Minerals* 16, 774-782.

Back Cover:
field trip itinerary

FIELD TRIP MAP

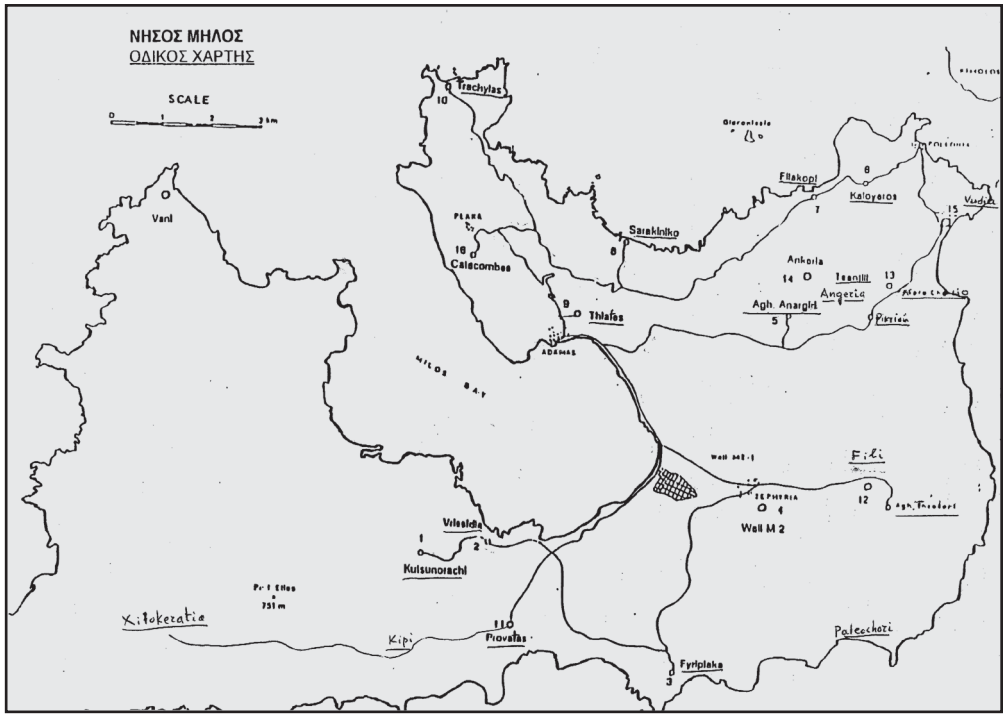

32nd INTERNATIONAL GEOLOGICAL CONGRESS

Edited by APAT